CCL28 modulates neutrophil responses and impacts the trajectory of mucosal infections.

Araceli Perez-Lopez[1,2,3], Steven Silva[1], Nicholas Dillon[1], Stephanie L. Brandt[1], Romana R. Gerner[1], Michael H. Lee[1], Karine Melchior[1], Jiram Torres-Ruiz[4,5], Victor A. Sosa-Hernandez[6,7], Rodrigo Cervantes-Diaz[6,7], Alfredo Perez-Fragoso[4], Sandra Romero-Ramirez[6,8], Diana Gomez-Martin[4], Jose L. Maravillas-Montero[6], Sean-Paul Nuccio[1,2], Victor Nizet[1,9,10], and Manuela Raffatellu[1,2,10,11*]

[1] Division of Host-Microbe Systems & Therapeutics, Department of Pediatrics, University of California San Diego, La Jolla, CA 92093, USA

[2] Department of Microbiology and Molecular Genetics, University of California Irvine, Irvine, CA 92697, USA

[3] Biomedicine Research Unit, Facultad de Estudios Superiores Iztacala, Universidad Nacional Autónoma de México. Tlalnepantla, State of México 54090, México.

[4] Department of Immunology and Rheumatology, Instituto Nacional de Ciencias Médicas y Nutrición Salvador Zubirán. México City 14080, México

[5] Emergency Medicine Department, Instituto Nacional de Ciencias Médicas y Nutrición Salvador Zubirán. Mexico City 14080, México

[6] Red de Apoyo a la Investigación, Universidad Nacional Autónoma de México and Instituto Nacional de Ciencias Médicas y Nutrición Salvador Zubirán, Mexico City 14080, México

[7] Departamento de Biomedicina Molecular, Centro de Investigación y de Estudios Avanzados del Instituto Politécnico Nacional, Mexico City 07360, Mexico

[8] Facultad de Medicina, Universidad Nacional Autónoma de México, Mexico City 04510, Mexico

[9] Skaggs School of Pharmacy and Pharmaceutical Sciences, University of California San Diego, La Jolla, CA, 92093, USA

[10] Center for Microbiome Innovation, University of California San Diego, La Jolla, CA 92093, USA

[11] Chiba University-UC San Diego Center for Mucosal Immunology, Allergy, and Vaccines (CU-UCSD cMAV), La Jolla, CA 92093, USA

*To whom correspondence should be addressed:
Manuela Raffatellu - Email: manuelar@ucsd.edu

Summary

The mucosal chemokine CCL28 is highly upregulated during infection but its role in this context is not well understood. Utilizing *Ccl28*$^{-/-}$ mice, we discovered that CCL28 promotes neutrophil recruitment to the infected mucosa. Neutrophils from these tissues expressed the CCL28 receptor CCR3, and CCR3 stimulation enhanced neutrophil antimicrobial activity against *Salmonella*. Moreover, bone marrow neutrophils harbored pre-formed intracellular CCR3 that was rapidly mobilized to the cell surface following phagocytosis or inflammatory stimuli. The functional consequences of CCL28 deficiency were strikingly different between two infection models, as *Ccl28*$^{-/-}$ mice were highly susceptible to *Salmonella* gut infection, but highly resistant to otherwise lethal *Acinetobacter* lung infection. CCL28 thus plays a critical role in the immune response to mucosal pathogens by regulating neutrophil recruitment and activation, a response whose ultimate consequence ranges from beneficial (control of the pathogen) to exceedingly negative (death of the host), depending on the infectious agent and impacted organs.

Introduction

Chemokines comprise a family of small chemoattractant proteins that play important roles in diverse host processes including chemotaxis, immune cell development, leukocyte activation and effector functions, tumor growth, and metastasis (Charo and Ransohoff, 2006; Zlotnik and Yoshie, 2000; Zlotnik et al., 2011). The chemokine superfamily includes 48 human ligands and 19 receptors, commonly classified into subfamilies (CC, CXC, C, and CX_3C) depending on the location of the cysteines in their sequence (Hughes and Nibbs, 2018; Nomiyama et al., 2013). Four chemokines predominate in mucosal tissues: CCL25, CCL28, CXCL14, and CXCL17 (Hernández-Ruiz and Zlotnik, 2017).

CCL28, also known as Mucosae-associated Epithelial Chemokine (MEC), belongs to the CC (or β-chemokine) subclass, and is constitutively produced in mucosal tissues including the digestive system, respiratory tract, and female reproductive system (Mohan et al., 2017). Although best studied for its homeostatic functions, CCL28 can also be induced under inflammatory conditions and is thus considered a dual function (homeostatic and inflammatory) chemokine (Mohan et al., 2017).

CCL28 signals via two receptors: CCR3 and CCR10 (Pan et al., 2000). During homeostasis in mice, CCL28 provides a chemotactic gradient for $CCR10^+$ B and T cells and guides the migration of $CCR10^+$ IgA plasmablasts to the mammary gland and other tissues (Burkhardt et al., 2019; Matsuo et al., 2018; Mohan et al., 2017). In a disease context, CCL28 has been best studied in allergic airway inflammation. High CCL28 levels are present in airway biopsies from asthma patients (O'Gorman et al., 2005), and $CCR3^+$ and $CCR10^+$ cells are recruited to the airways in a CCL28-dependent fashion in murine asthma models (English et al., 2006; John et al., 2005). Recently, CCL28 was noted to be highly induced in adult patients with severe disease and organ damage stemming from SARS-CoV-2 infection (COVID-19) and children with COVID-19-associated multisystem inflammatory syndrome (Gruber et al., 2020; Yan Yan et al., 2020).

In the human gut, CCL28 is upregulated during inflammation of the gastric mucosa in *Helicobacter pylori*-infected patients (Hansson et al., 2008) and in the colon of patients with ulcerative colitis, an important form of inflammatory bowel disease (Lee et al., 2020a; Ogawa et al., 2004). In the mouse gut, CCL28 production is increased in the dextran sulfate sodium (DSS) model of colitis (Matsuo et al., 2018). Epithelial cells are an important source of CCL28 (Lee et al., 2020a; Ogawa et al., 2004), and its expression can be induced by stimulation of cultured airway or intestinal epithelial cells with the proinflammatory cytokines IL-1α, IL-1β, or TNFα, or following *Salmonella* infection of cultured HCA-7 colon carcinoma cells (Ogawa et al., 2004).

Collectively, a variety of studies have postulated that CCL28 is an important chemokine for inflammatory diseases ranging from asthma to ulcerative colitis, and during the immune response to infection with bacterial or viral pathogens. Yet, CCL28 function in health and disease remains understudied, largely because *Ccl28*$^{-/-}$ mice have only recently been described (Burkhardt et al., 2019; Matsuo et al., 2018). Here, we investigate the function and underlying mechanism of CCL28 during the mucosal response to infection.

By comparing infection in *Ccl28*$^{-/-}$ mice and their wild-type littermates, we discovered a key role for CCL28 in promoting the migration and/or retention of neutrophils to the gut during infection with *Salmonella enterica* serovar Typhimurium (*S.* Typhimurium), and to the lung during infection with multidrug-resistant *Acinetobacter baumannii*. Although the host responses modulated by CCL28 are similar in the gut and in the lung mucosa, we observed striking differences between the functional consequences of CCL28 deficiency in a gut infection model and a lung infection model. We conclude that the CCL28/CCR3 axis plays a critical role in the innate immune response to mucosal pathogens by regulating neutrophil recruitment and activation, a response whose ultimate outcome ranges from beneficial (control of the pathogen) to exceedingly negative (death of the host), depending on the infectious agent and impacted organs.

Results

CCL28-mediated responses limit *Salmonella* gut colonization and systemic dissemination.

CCL28 is constitutively produced by many mucosal tissues and further upregulated during inflammation (Hansson et al., 2008; Lee et al., 2020a; Ogawa et al., 2004). To study the role of CCL28 during gastrointestinal infection, we utilized the enteric pathogen *S*. Typhimurium and the well-established streptomycin-treated C57BL/6 mouse model of colitis (Barthel et al., 2003). At 96h post-infection with *S*. Typhimurium we observed an ~4-fold increase of CCL28 by ELISA

analysis of feces from wild-type mice relative to uninfected controls (**Fig. 1A**). In a preliminary characterization, *Ccl28*$^{-/-}$ mice infected with *S*. Typhimurium exhibited increased lethality compared to their wild-type littermates beginning at 24h post-infection (Burkhardt et al., 2019). As such, we enumerated *S*. Typhimurium colony-forming units (CFU) in tissues at 72h post-infection, instead of the frequently studied 96h endpoint. We recovered significantly higher *S*. Typhimurium CFU from the gastrointestinal tract (cecum content, Peyer's patches), the mesenteric lymph nodes, and systemic sites (bone marrow and spleen) of *Ccl28*$^{-/-}$ mice vs. wild-type littermates (**Fig. 1B**), demonstrating that the chemokine is an essential component of host defense against *S*. Typhimurium in this colitis model. When bypassing the gut by infecting mice with *S*. Typhimurium via the intraperitoneal route, we also observed an ~4-fold increase of CCL28 in the serum (**Suppl. Fig. 1A**); however, we recovered equal numbers of *S*. Typhimurium CFU in the spleen, liver, and blood of wild-type and *Ccl28*$^{-/-}$ mice (**Suppl. Fig. 1B**). Taken together, these results indicate that CCL28 helps the host to control *S*. Typhimurium infection at its point of origin in the gut mucosa, prompting us to further investigate the underlying mechanisms of CCL28-mediated mucosal protection.

CCL28 promotes neutrophil recruitment/retention to the gut during *Salmonella* infection.

During homeostasis, CCL28 has chemotactic activity in the gut mucosa towards $CD4^+$ and $CD8^+$ T cells and IgA-producing B cells (Burkhardt et al., 2019; Matsuo et al., 2018; Mohan et al., 2017). However, we found that B and T cell numbers in the intestine of wild-type and *Ccl28*$^{-/-}$ mice were similar during homeostasis (**Suppl. Fig. 2A** and **2C**) and 48h after *S*. Typhimurium infection (**Suppl. Fig. 2B** and **2D**), indicating that the chemokine's protective role is likely independent of its B or T cell chemotactic activity. A second role attributed to CCL28 is a direct antimicrobial activity against some bacteria (e.g., *Streptococcus mutans* and *Pseudomonas aeruginosa*) and fungi (e.g., *Candida albicans*) (Hieshima et al., 2003). However, we found that *S.* Typhimurium is not susceptible to CCL28's antimicrobial activity *in vitro* (**Suppl. Fig. 1C, D**).

Neutrophils are a crucial component of the host response to *S.* Typhimurium (reviewed in (Perez-Lopez et al., 2016)), and neutropenia increases the severity of infection with non-typhoidal *Salmonella* in both mice and humans (Bhatti et al., 1998; Fierer, 2001; Vassiloyanakopoulos et al., 1998; Yaman et al., 2018). Strikingly, we found that ~50% fewer neutrophils ($CD11b^+$ $Ly6G^+$ cells) were recruited to the gut of *Ccl28*$^{-/-}$ mice 48h after *S.* Typhimurium infection relative to their wild-type littermates (**Fig. 1C, D**). Commensurate with this finding, neutrophil counts in the blood of infected *Ccl28*$^{-/-}$ mice were increased compared to wild-type mice (**Fig. 1C, D**), indicating a defect in recruitment of circulating neutrophils to the site of infection. Neutrophil counts in the bone marrow were similar between wild-type and *Ccl28*$^{-/-}$ animals (**Fig. 1C, D**), excluding a defect in granulopoiesis. Likewise, bone marrow and blood neutrophil counts were similar in wild-type and *Ccl28*$^{-/-}$ mice under homeostatic conditions (**Suppl. Fig. 2E, F**) and neutrophils were not found in uninfected gut tissue (data not shown). Thus, CCL28 promotes recruitment and/or retention of neutrophils to the gut during *S.* Typhimurium infection by a mechanism that transpires after bone marrow neutrophil production and their egress into the blood circulation.

Gut proinflammatory gene expression and tissue pathology are reduced in *Ccl28*$^{-/-}$ mice.

Neutrophils can mediate inflammation by directly producing proinflammatory molecules or by engaging in crosstalk with other cells (Sabroe et al., 2005). We evaluated the expression of genes encoding proinflammatory cytokines in the cecum of *Ccl28*$^{-/-}$ mice and their wild-type littermates 72h after *S.* Typhimurium infection. IFNγ and IL-1β gene transcripts were significantly higher in the cecum of infected wild-type mice vs. *Ccl28*$^{-/-}$ mice, while expression of genes encoding other factors involved in neutrophil recruitment (CXCL1, GM-CSF, IL-17A) or the proinflammatory cytokine TNF-α did not differ significantly (**Fig. 1E**). No difference in the expression of these genes was found between uninfected wild-type mice and *Ccl28*$^{-/-}$ mice (data not shown). Consistent with the role of neutrophils as important mediators of inflammation in *S.*

Typhimurium colitis, histopathology at 72h post-infection revealed marked cecal inflammation in wild-type mice that was greatly reduced in *Ccl28*$^{-/-}$ mice (**Fig. 1F-H**). Thus, by modulating the recruitment/retention of neutrophils to the infected gut, CCL28 promotes the development of inflammatory tissue pathology and colitis during *S*. Typhimurium infection.

Gut neutrophils express receptors CCR3 and CCR10 during *Salmonella* infection

CCL28 attracts leukocytes that express at least one of its receptors (CCR3, CCR10). Eosinophils express CCR3, whereas CCR10 is found on T cells, B cells, and IgA-secreting plasma cells (Mohan et al., 2017). Although early studies concluded that CCR3 was a marker of eosinophils but absent in neutrophils (Höchstetter et al., 2000), the receptor was later detected on the surface of neutrophils isolated from patients with chronic inflammation (Hartl et al., 2008). Based on our findings of CCL28-dependent neutrophil recruitment to the gut during enteric infection (**Fig. 1**), we performed flow cytometry on single-cell suspensions from the gut, blood, and bone marrow of mice infected with *S*. Typhimurium to study surface expression of CCR3 and CCR10. While both chemokine receptors were identified on a subset of bone marrow neutrophils (36% CCR3, 12% CCR10) and blood neutrophils (25% CCR3, 16% CCR10) during infection, neutrophils expressing these receptors were enriched in the inflamed gut, with ~80% expressing CCR3 and ~28% expressing CCR10 (**Fig. 2A**, **B**). In a separate experiment where neutrophils were simultaneously stained for both CCR3 and CCR10, ~35% of gut neutrophils from infected wild-type mice expressed both receptors (**Suppl. Fig. 3A)**, and infected *Ccl28*$^{-/-}$ mice expressed similar levels of these receptors as wild-type mice (**Suppl. Fig. 3B)**. Thus, neutrophil expression of a CCL28 receptor, particularly CCR3, appears to facilitate recruitment and/or retention to the gut during *S*. Typhimurium colitis.

Proinflammatory stimuli and phagocytosis induce expression of CCR3 and CCR10 on neutrophils

We next investigated potential mechanisms underpinning the upregulation of CCR3 and CCR10 in neutrophils. A prior study indicated that a cocktail of proinflammatory cytokines (GM-CSF, IFNγ, TNFα) boosted CCR3 expression in human peripheral blood mononuclear cells (PBMCs) from healthy donors (Hartl et al., 2008) expression of these cytokines is highly induced during *S.* Typhimurium colitis (**Fig. 1E**). We thus stimulated bone marrow neutrophils from wild-type mice (which express low levels of CCR3 and CCR10) with these cytokines (alone or in combination), or with lipopolysaccharide (LPS), with the protein kinase C activator phorbol 12-myristate 13-acetate (PMA), or with the N-formylated, bacterial-derived chemotactic peptide fMLP. Treatment of neutrophils with the GM-CSF + IFNγ + TNFα cytokine combination or with LPS induced higher CCR3 (~40% positive cells) and CCR10 (~20% positive cells) expression, whereas PMA and fMLP separately yielded more modest yet significant induction (**Fig. 2C, D** and **Suppl. Fig. 4A, B**).

Phagocytosis of microbes and necrotic debris are critical neutrophil functions at tissue foci of infection and inflammation (Uribe-Querol and Rosales, 2020), and gene expression changes are observed in human neutrophils following phagocytosis (Kobayashi et al., 2002). We thus tested whether CCR3 and CCR10 were induced by phagocytosis, incubating bone marrow neutrophils with latex beads, with or without the aforementioned cytokine cocktail. Although phagocytosis of latex beads alone did not significantly induce neutrophil CCR3 receptor expression (~7% of neutrophils), latex beads augmented cytokine cocktail-induced CCR3 expression (~53% of neutrophils vs. ~30% with cocktail alone; **Fig. 2E**). This synergistic effect of phagocytosis was not noted for CCR10 (**Fig. 2F**).

To further probe the role of phagocytosis in CCR3 expression, we incubated bone marrow neutrophils with live *S.* Typhimurium for 1h. We found that *S.* Typhimurium rapidly induced the expression of CCR3 on the neutrophil surface (~80% of cells; **Fig. 2G**), whereas CCR10 was only minimally induced (**Fig. 2H**). To confirm that phagocytosis of bacteria was responsible for inducing receptor expression, the assay was repeated with cytochalasin D, a potent inhibitor of the actin polymerization required for phagocytic uptake, or with vehicle alone (DMSO). Whereas ~60% of bone marrow neutrophils became $CCR3^+$ within 1h of *S.* Typhimurium infection, this induction was largely blocked by cytochalasin D (**Fig. 2I**); and while CCR10 was expressed in ~4% of neutrophils following infection, cytochalasin D exhibited a similar inhibitory effect on its expression (**Fig. 2J**). Proinflammatory stimuli and phagocytosis thus enhance the expression of CCR3 and, to a lesser extent, CCR10, on the neutrophil surface.

CCR3 is stored intracellularly in neutrophils

Neutrophil intracellular compartments and granules harbor enzymes, cytokines, and receptors that are required for rapid responses to pathogens. For example, activation of human neutrophils induces a rapid translocation of complement receptor type 1 (CR1) from an intracellular compartment to the cell surface, increasing its surface expression up to 10-fold (Berger et al., 1991).

As we detected a rapid (within 1h) increase of neutrophil CCR3 surface expression upon *S.* Typhimurium infection, we hypothesized that CCR3, akin to CR1, may be stored in a neutrophil intracellular compartment, consistent with reports of intracellular CCR3 in eosinophils (Spencer et al., 2006). We found that uninfected bone marrow neutrophils express relatively low surface levels of CCR3 (**Fig. 3A**), but when permeabilized for intracellular staining, most (~85%) were $CCR3^+$, indicating that CCR3 is stored intracellularly (**Fig. 3B**). Upon *S.* Typhimurium infection *in vitro*, bone marrow neutrophils rapidly increased CCR3 surface expression (**Fig. 3A**), consistent

with a mobilization of pre-formed receptor from an intracellular compartment (**Fig. 3B**). Intracellular stores of CCR10 were not detected in bone marrow neutrophils under homeostatic conditions nor during *S.* Typhimurium infection (**Suppl. Fig. 4C**). Neutrophils from bone marrow, blood, and gut tissue of mice orally infected with *S.* Typhimurium harbored both intracellular and surface CCR3, albeit at differing levels (**Fig. 3C**). We conclude that CCR3 is present intracellularly in neutrophils and quickly mobilized to the cell surface upon infection, phagocytosis, and/or cytokine stimulation.

Contributions of CCL28 to neutrophil chemotaxis and antimicrobial activity

Chemokines are essential for neutrophil migration to sites of infection and may regulate additional neutrophil bactericidal effector functions including the production of reactive oxygen species (ROS), release of antimicrobial peptides, and formation of neutrophil extracellular traps (NETs) (Capucetti et al., 2020). We tested if CCL28 has chemotactic and/or immunostimulatory activity towards bone marrow neutrophils *in vitro* after boosting their CCR3 surface expression with the cytokine cocktail (GM-CSF + IFNγ + TNFα) shown in **Fig. 2**. We incubated the neutrophils either with CCL28, or with the well-known neutrophil chemoattractant CXCL1, or with CCL11/eotaxin (a chemokine that binds CCR3 and is induced in the asthmatic lung to promote eosinophil recruitment (Conroy and Williams, 2001; Garcia-Zepeda et al., 1996; Kitaura et al., 1996)). We found CCL28 promoted neutrophil chemotaxis, though not as potently as CXCL1, while CCL11 had no significant effect (**Fig. 3D**).

To test whether CCL28 stimulation enhanced neutrophil effector function, we incubated *S.* Typhimurium with bone marrow neutrophils for 2.5h with or without CCL28 or CCL11, then quantified bacterial killing. Stimulation with CCL28 strongly increased neutrophil bactericidal activity against *S.* Typhimurium, with clearance of ~40% of the bacterial inoculum, compared to

only ~10% clearance seen with unstimulated neutrophils (**Fig. 3E**). Neutrophils stimulated with CCL11 displayed an intermediate phenotype (~25% bacterial killing). Corroborating receptor specificity, the CCL28-mediated increase in neutrophil bactericidal activity was reversed in the presence of the small molecule SB328437, a CCR3 antagonist (White et al., 2000) (**Fig. 3F**). Similarly, SB328437 also reversed the effect of CCL11 on neutrophil bactericidal activity (**Fig. 3F**). Together, these results demonstrate that CCL28 boosts neutrophil effector function in a CCR3-dependent manner.

Ccl28$^{-/-}$ mice are protected from lethal infection in an *Acinetobacter* pneumonia model

CCL28 is expressed in several mucosal tissues beyond the gut, including the lung (Mohan et al., 2017). To investigate if CCL28 mediates neutrophil recruitment and host protection during lung infection, we employed a murine *Acinetobacter baumannii* pneumonia model *(Dillon et al., 2019; Lin et al., 2015)*. *A. baumannii* is an emerging, frequently multidrug-resistant Gram-negative pathogen that causes potentially lethal nosocomial pneumonia in intensive care unit patients (Ayoub Moubareck and Hammoudi Halat, 2020). Following intratracheal *A. baumannii* infection, we observed a striking and unexpected phenotype in the mortality curves of wild-type vs. *Ccl28*$^{-/-}$ mice: while 6 out of 8 wild-type littermates (75%) died within 48h, 7 out of 8 of the *Ccl28*$^{-/-}$ knockout mice (88%) survived through Day 10 post-infection (**Fig. 4A**). The enhanced resistance of *Ccl28*$^{-/-}$ mice relative to their wild-type littermates was not associated with a significant reduction in *A. baumannii* CFU recovered from bronchoalveolar lavage (BAL) fluid or blood (**Fig. 4B, C**). Thus, opposite to what we observed during *S*. Typhimurium gut infection, CCL28 did not confer protection during *A. baumannii* lung infection, but rather exacerbated lethality.

CCL28 promotes neutrophil recruitment/retention to the lung during *Acinetobacter* infection

Prior studies demonstrated that neutrophils are recruited to the lungs of mice infected with *A. baumannii* beginning at 4h post-infection, and peak at 24h post-infection (Tsuchiya et al., 2012; Van Faassen et al., 2007). As CCL28 contributed to neutrophil recruitment during *S*. Typhimurium gut infection, we analyzed neutrophil recruitment to the lung mucosa 24h after *A. baumannii* infection in wild-type and *Ccl28*$^{-/-}$ mice. BAL fluid showed a significantly greater cellular infiltrate (largely comprised of neutrophils; CD11b^{+} Ly6G^{+} cells) in wild-type mice than in *Ccl28*$^{-/-}$ littermates (**Fig. 4D-F**). A similar higher percentage of neutrophils was identified in lung tissue of wild-type mice compared to *Ccl28*$^{-/-}$ mice post-infection, whereas we found no differences in neutrophil numbers in the blood or bone marrow (**Fig. 4E-F**). Although histopathology of lung tissue revealed substantial lung inflammation in both wild-type and *Ccl28*$^{-/-}$ mice after *A. baumannii* infection (**Supp. Fig 5**), immunofluorescence analysis revealed remarkable differences in the composition of the cellular infiltrate — lungs from infected wild-type mice showed an abundant infiltrate of neutrophils (Ly6G^{+} cells) that was significantly reduced in *Ccl28*$^{-/-}$ mice (**Fig. 4G-H** and **Supp. Fig 5**).

Comparable to what we observed during *S*. Typhimurium gut infection, induction of the genes encoding IFNγ and IL-1β was significantly lower in *A. baumannii*-infected lungs of *Ccl28*$^{-/-}$ mice relative to wild-type mice (**Fig. 4I**). By contrast, expression of the *Cxcl1* gene was reduced, whereas the other proinflammatory genes tested (*Il17a*, *Csf2*, *Tnfa*) did not differ between the groups (**Fig. 4I**). CCL28 thus contributes to lung inflammation and neutrophil recruitment/retention during *A. baumannii* pneumonia.

Lung neutrophils express receptors CCR3 and CCR10 during *Acinetobacter* infection

As with neutrophils isolated from the gut of wild-type mice infected with *S.* Typhimurium, neutrophils isolated from the BAL of *A. baumannii*-infected wild-type mice were positive for CCR3 and CCR10 surface expression, with ~73% of neutrophils expressing CCR3 (**Fig. 5A**) and ~43% expressing CCR10 (**Fig. 5B**). In a separate experiment where neutrophils were simultaneously stained for both CCR3 and CCR10, ~20% of BAL neutrophils from infected wild-type mice expressed both receptors (**Suppl. Fig. 3C)**, and infected *Ccl28*$^{-/-}$ mice expressed similar levels of these receptors as wild-type mice (**Suppl. Fig. 3D)**. As predicted, a lower percentage of neutrophils isolated from the blood and the bone marrow of mice infected with *A. baumannii* were positive for the receptors (**Fig. 5A, 5B**). Moreover, neutrophils isolated from all of these locations harbored CCR3 intracellularly, and surface expression levels were higher on neutrophils isolated from the BAL relative to other sites (**Fig. 5C**).

In vitro infection with *A. baumannii* rapidly induced surface expression of CCR3 on neutrophils (**Fig. 5D**), although the induction was smaller than that observed with *S.* Typhimurium (**Fig. 2G**). In contrast to findings with *S.* Typhimurium, *ex vivo* neutrophil killing of *A. baumannii* was not significantly enhanced by CCL28 or CCL11 treatment (**Fig. 5E**). Taken together, our results indicate that CCL28 modulates host responses in the lung, including the recruitment of neutrophils, during *A. baumannii* infection. However, CCL28 is not protective in this context, in part because the CCL28-mediated influx of neutrophils (**Fig. 4D-H** and **Supp. Fig. 5**) fails to reduce pathogen burden (**Fig. 4B,C**).

CCR3 and CCR10 are highly induced in neutrophils isolated from COVID-19 patients

We next sought to determine whether our findings in the mouse model could be evidenced in humans. At this point in our study (mid-2020), infection with SARS-CoV-2 had become a global pandemic, and predominated among patients hospitalized with an infection. A subset of COVID-

19 patients progress to severe disease with pneumonia and organ damage. Such patients typically exhibit a marked increase of neutrophils, accompanied in the most severe cases by an increased neutrophil to lymphocyte ratio (Fu et al., 2020). SARS-CoV-2 also induces the formation of neutrophil extracellular traps (NETs) that further exacerbate inflammatory pathology (Veras et al., 2020). These characteristic findings gave us a window to investigate whether CCR3 and CCR10 are expressed on the surface of neutrophils in human patients with severe COVID-19 disease including those in critical condition (see recruitment criteria in the materials and methods).

Consistent with the aforementioned reports, both severe and critical COVID-19 patients exhibited a marked increase in the percentage of blood neutrophils relative to healthy controls (**Supp. Fig. 6A**). Neutrophils from both groups of COVID-19 patients exhibited low surface expression of L-selectin (CD62L; **Supp. Fig. 6B**), indicating that these cells were activated. In healthy controls, only a small percentage of neutrophils (fewer than ~4%) expressed CCR3 and CCR10 on their surface (**Supp. Fig. 6C,D**). In contrast, patients with severe COVID-19 showed a significant upregulation of surface CCR3 and, to a lesser extent, CCR10 (**Supp. Fig. 6C,D**). Analysis of clinical parameters for COVID-19 patients revealed that the percentage of $CCR3^{+}$ neutrophils correlated with many markers of disease severity, including higher respiratory frequency, elevated prothrombin time, and D dimer (**Supp. Fig. 6E, F**). Thus, neutrophils isolated from COVID-19 patients express CCR3 and CCR10 on their surface, indicating that these receptors are indeed present on neutrophils during human disease.

Discussion

The mucosal immune response serves to maintain tissue homeostasis and to protect the host against invading pathogens. Here we discovered that the chemokine CCL28 recruits

353 neutrophils to the mucosa, a response that was protective during gastrointestinal infection with
354 *Salmonella*, but detrimental during lung infection with *Acinetobacter*.

355 Consistent with our initial observation that *Ccl28*$^{-/-}$ mice exhibit higher lethality during *S.*
356 Typhimurium infection (Burkhardt et al., 2019), we found higher intestinal colonization and
357 dissemination of *S.* Typhimurium in *Ccl28*$^{-/-}$ mice than their wild-type littermates. This beneficial
358 role for CCL28 was negligible when the pathogen was inoculated intraperitoneally to bypass the
359 gut mucosa. Although it has been reported that CCL28 exerts direct antimicrobial activity against
360 some bacteria and fungi (Hieshima et al., 2003), the chemokine does not directly inhibit
361 *Salmonella in vitro*. Moreover, even though the CCL28 receptors CCR3 and CCR10 are
362 expressed on eosinophils and on B and T cells (Höchstetter et al., 2000; Pan et al., 2000; Wang
363 et al., 2000), none of these cell types appeared to be responsible for the observed protective role
364 of CCL28 during *Salmonella* infection. Eosinophils are not a major component of the host
365 response to *Salmonella*, and we observed comparable numbers of B and T cells in the gut during
366 homeostasis, as well as during *Salmonella* infection, in wild-type and *Ccl28*$^{-/-}$ mice.

367 Neutrophils are a hallmark of inflammatory diarrhea. In the *Salmonella* colitis model,
368 neutrophils are rapidly recruited to the gut following infection. We found that neutrophil numbers
369 were significantly reduced in the mucosa of infected *Ccl28*$^{-/-}$ mice relative to wild-type mice,
370 thereby identifying CCL28 as a key factor for neutrophil recruitment/retention during infection.
371 Neutrophils migrate from the bone marrow to the blood to infected sites following a chemokine
372 gradient (Capucetti et al., 2020), and express chemokine receptors CXCR1, CXCR2, CXCR4 and
373 CCR2, as well as CCR1 and CCR6 under certain circumstances (Kobayashi, 2008). CXCR2 is a
374 promiscuous receptor that binds to the chemokines CXCL1, 2, 3, 5, 6, 7, and 8 (Ahuja and
375 Murphy, 1996), whereas CXCR1 only binds CXCL6 and CXCL8 (Capucetti et al., 2020).
376 Activation of CXCR2 induces mobilization of neutrophils from the bone marrow to the bloodstream
377 and participates in the release of NETs (Marcos et al., 2010). Engagement of CXCR1 and CXCR2

also triggers signaling pathways resulting in the production of cytokines and chemokines that amplify neutrophil responses (Sabroe et al., 2005). Following extravasation to the site of infection, neutrophils downregulate CXCR2 and upregulate CCR1, 2, and 5, which cumulatively boosts neutrophil ROS production and phagocytic activity (Capucetti et al., 2020). Our results indicate that CCL28 contributes to neutrophil migration and activation, and that its receptors CCR3 and CCR10 are upregulated in the mucosa during infection, where ~80% of neutrophils express surface CCR3.

Although an initial study concluded CCR3 was absent on neutrophils (Höchstetter et al., 2000), two subsequent studies reported CCR3 expression on human neutrophils isolated from the lung of patients with chronic lung disease (Hartl et al., 2008) and on neutrophils isolated from the BAL of mice infected with influenza (Rudd et al., 2019). CCR10 expression in neutrophils has not been previously reported. Our study demonstrates that a substantial number of neutrophils isolated from infected mucosal sites express CCR3 as well as CCR10 on their surface, whereas in healthy humans and mice the vast majority of neutrophils do not express these receptors on their surface. As we detected CCR3 on the neutrophil surface quite rapidly after infection, we predicted that the receptor was stored in intracellular compartments, akin to what was found in eosinophils (Spencer et al., 2006). Indeed, neutrophils isolated from bone marrow, blood, and infected mucosal tissue were all positive for CCR3 intracellular staining, and we could recapitulate the increase of surface receptor expression *in vitro* by incubating bone marrow neutrophils with proinflammatory stimuli (LPS, or the cytokines GM-CSF + IFNγ + TNFα), or following phagocytosis of bacterial pathogens. In all cases, upregulation of surface CCR3 on neutrophils was more robust than that of CCR10. CCL28 stimulation of bone marrow neutrophils *in vitro* increased their antimicrobial activity against *Salmonella*, which was reverted by the addition of a CCR3 antagonist. These results were consistent with the *in vivo* data showing reduced *Salmonella* colonization in wild-type mice.

403 The lung, possessing a thin, single-cell alveolar layer to promote gas exchange, may be
404 less resilient than the intestine to neutrophil inflammation before losing barrier integrity and critical
405 functions. Thus, insufficient neutrophil recruitment can lead to life-threatening infection, whereas
406 extreme accumulation of neutrophils can result in excessive inflammatory lung injury (Craig et al.,
407 2009). In the *Acinetobacter* pneumonia model, *Ccl28*$^{-/-}$ mice exhibit a marked reduction in the
408 number of neutrophils in the BAL and in the lung. However, in stark contrast to *Salmonella*
409 infection, *Ccl28*$^{-/-}$ mice were protected during *A. baumannii* pneumonia. Most *Ccl28*$^{-/-}$ mice
410 survived until the experiment's arbitrary endpoint at Day 10 post-infection, whereas nearly all wild-
411 type littermates succumbed by Day 2. In contrast to *Salmonella*, stimulation with CCL28 did not
412 enhance neutrophil antimicrobial activity against *Acinetobacter*. Moreover, the high survival of
413 *Ccl28*$^{-/-}$ mice infected with *A. baumannii* indicates that CCL28 can play a detrimental role for the
414 host during pulmonary infection. While functioning neutrophils have been described to play a role
415 in controlling *Acinetobacter* infection (García-Patiño et al., 2017; Grguric-Smith et al., 2015; Van
416 Faassen et al., 2007), an exaggeration of neutrophil recruitment to the *Acinetobacter*-infected
417 lung is deleterious (Yamada et al., 2013; Zeng et al., 2019, 2020). For example, in one relevant
418 *Acinetobacter* pneumonia study, depletion of alveolar macrophages increased neutrophil
419 infiltration, promoted extensive tissue damage, and increased systemic dissemination of
420 *Acinetobacter* (Lee et al., 2020b).

421 Our findings highlight the fact that the impact of the host response to infection can be
422 context dependent, and that some immune components mediate different outcomes in the gut
423 and in the lung. For example, neutrophil recruitment to the gut via CXCR2 has a protective effect
424 during *Salmonella* infection (Marchelletta et al., 2015). In contrast, *Cxcr2*$^{-/-}$ mice are protected
425 during lung infection with *Mycobacterium tuberculosis*, due to reduced neutrophil recruitment and
426 reduced pulmonary inflammation (Nouailles et al., 2014). Thus, CCL28-dependent modulation of
427 neutrophil recruitment/retention during infection, and activation of CCR3 and/or CCR10, are

428 protective or detrimental depending on the pathogen and on the site of infection. Consistent with
429 this notion, an increase in circulating neutrophils is associated with severe disease in COVID-19
430 patients, where neutrophils contribute to lung and tissue damage (Veras et al., 2020). In our
431 patient cohort, CCR3 and CCR10 surface expression on blood neutrophils was increased relative
432 to healthy controls, which correlated with disease severity. Although we did not have access to
433 BAL or lung tissue, it is possible that CCR3 and CCR10 expression may even be higher in
434 neutrophils at these sites, similar to our observations in animal models of infection.

435 Altogether, this study demonstrates that CCL28 plays an important role in the mucosal
436 response to pathogens through the recruitment of neutrophils to the site of infection and through
437 the activation of CCR3. These findings could have implications for other infectious and non-
438 infectious diseases where neutrophil recruitment plays a major role, and may lead to the
439 identification of new CCL28-targeted therapies to modulate neutrophil function and mitigate
440 collateral damage.

441

442 **Materials and methods**

443 **Generation and breeding of *Ccl28*$^{-/-}$ mice**

444 The first colony of *Ccl28*$^{-/-}$ mice was described in a prior manuscript (Burkhardt et al., 2019) and
445 used for initial studies at UC Irvine. At UC San Diego, we generated a new colony of *Ccl28*$^{-/-}$ mice
446 with Cyagen Biosciences (Santa Clara, California), using CRISPR/CAS9 technology. Exons 1
447 and 3 were selected as target sites, and two pairs of gRNA targeting vectors were constructed
448 and confirmed by sequencing. The gRNA and Cas9 mRNA were generated by *in vitro*
449 transcription, then co-injected into fertilized eggs for knockout mouse production. The resulting
450 pups (F0 founders) were genotyped by PCR and confirmed by sequencing. F0 founders were

bred to wild-type mice to test germline transmission and for F1 animal generation. Tail genotyping of offspring was performed using the following primers:

F: 5'-TCATATACAGCACCTCACTCTTGCCC-3', R: 5'-GCCTCTCAAAGTCATGCCAGAGTC-3' and He/Wt-R: 5'-TCCCGGCCTTGAGTATGTTAGGC-3'. The expected product size for the wild-type allele is 466 bp and for the knockout allele is 700 bp.

All mouse experiments were conducted with cohoused wild-type and *Ccl28*$^{-/-}$ littermate mice, and were reviewed and approved by the Institutional Animal Care and Use Committees at UC Irvine and UC San Diego.

Salmonella infection models

For the *Salmonella* colitis model, 8-10 week-old male and female mice were orally gavaged with 20mg streptomycin 24h prior to oral gavage with 10^9 colony-forming units (CFU) of *Salmonella enterica* serovar Typhimurium strain IR715 (a fully virulent, nalidixic acid-resistant derivative of ATCC 14028s) (Stojiljkovic et al., 1995), as previously described (Barthel et al., 2003; Raffatellu et al., 2009). Mice were euthanized at 72h post-infection, then colon content, spleen, mesenteric lymph nodes, Peyer's patches, and bone marrow were collected, weighed, homogenized, serially diluted, and plated on Miller Lysogeny broth (LB) + Nal (50µg/mL) agar plates to enumerate *Salmonella* CFU. For the *Salmonella* bacteremia model, mice were injected intraperitoneally with 10^3 CFU. Mice were euthanized at 72h post-infection, then blood, spleen, and liver were collected to determine bacterial counts.

Acinetobacter infection model

For the murine pneumonia model**,** *Acinetobacter baumannii* strain AB5075 was cultured in Cation-Adjusted Mueller-Hinton Broth (CA-MHB) overnight, then subcultured the next day to an OD_{600} of ~0.4 ($1x10^8$ CFU/mL; mid-logarithmic phase). These cultures were centrifuged at 3202x*g*, the supernatant was removed, and pellets were resuspended and washed in an equal volume of 1x Dulbecco's PBS (DPBS) three times. The final pellet was resuspended in 1x DPBS to yield a suspension of 2.5×10^9 CFU/mL. Using an operating otoscope (Welch Allyn), mice under 100 mg/kg ketamine (Koetis) + 10 mg/kg xylazine (VetOne) anesthesia were inoculated intratracheally with 40 µL of the bacterial suspension (10^8 CFU/mouse). Post-infection mice were recovered on a sloped heating pad. For analysis of bacterial CFU, mice were sacrificed at 24h post-infection, the BAL was collected, and serial dilutions were plated on LB agar to enumerate bacteria (Dillon et al., 2019).

Blood samples from COVID-19 patients and healthy donors

Whole-blood samples were collected from COVID-19 patients and healthy donors that were recruited at a tertiary care center in Mexico City (Instituto Nacional de Ciencias Médicas y Nutrición Salvador Zubirán). Hospitalized patients with a positive qPCR test for SARS-CoV-2 on nasopharyngeal swab were invited to participate in the study. Patients were classified as "severe" or "critical" depending on the following disease severity criteria. Patients with severe illness displayed one or more of the following signs: respiratory failure, respiratory rate >30 bpm, oxygen saturation < 92% at rest, arterial partial pressure of oxygen (PaO_2)/fraction of inspired oxygen (FiO2) (PaO_2/FiO_2) ratio < 300 mmHg. Patients with critical illness displayed one or more of the following signs: requirement for mechanical ventilation, shock, or concomitant organ failure (Liu et al., 2020). Healthy controls and patients signed an informed consent form before inclusion in the study, and the protocol was approved by the Instituto Nacional de Ciencias Médicas y Nutrición Salvador Zubirán ethics and research committees (Ref. 3341) in compliance with the Helsinki declaration.

499

500 **CCL28 ELISA**

501 Fresh fecal samples were collected at 96h post-infection from wild-type mice. Fecal pellets were
502 weighed, resuspended in 1 mL of sterile PBS containing a protease inhibitor cocktail (Roche),
503 and incubated at room temperature shaking for 30 min. Samples were centrifuged at 9391x*g* for
504 10 min, supernatants were collected, then analyzed to quantify CCL28 using a sandwich ELISA
505 kit (BioLegend).

506

507 **Cell extraction and analysis**

508 For the *Salmonella* colitis model, the terminal ileum, cecum, and colon were collected and kept in
509 IMDM medium supplemented with 10% FBS and 1% antibiotic/antimycotic. Next, the Peyer's
510 patches were removed, and the intestinal fragments were cut open longitudinally and washed
511 with HBSS supplemented with 15 mM HEPES and 1% antibiotic/antimycotic. Then, the tissue
512 was shaken in 10 mL of an HBSS/ 15 mM HEPES/ 5 mM EDTA/ 10% FBS solution at 37 ºC in a
513 water bath for 15 min. The supernatant was removed and kept on ice. The remaining tissue was
514 cut into small pieces and digested in a 10 mL mixture of collagenase (Type VII, 1 mg/mL),
515 Liberase (20 µg/mL), and DNAse (0.25 mg/mL) in IMDM medium for 15 min in a shaking water
516 bath at 37 ºC. Afterwards, the supernatant and tissue fractions were strained through a 70 µm
517 cell strainer and pooled, and the extracted cells were used for flow cytometry staining. For the *A.*
518 *baumannii* infection model, the lungs were collected and processed as described for the gut. BAL
519 was collected, centrifuged, and pellets were washed with 1x PBS. The obtained cells were used
520 for flow cytometry staining. Briefly, cells were blocked with a CD16/32 antibody (Bio-Legend),
521 stained with the viability dye eFluor780 (Thermo Fisher), then extracellularly stained using the
522 following monoclonal antibodies: anti-mouse CD45 (clone 30-F11), anti-mouse CD3 (clone
523 17A2), anti-mouse CD4 (clone RM4-5), anti-mouse CD8α (clone 53-6.7), anti-mouse CD19 (clone

1D3/CD19), anti-mouse Ly6G (clone 1A8), anti-mouse CD11b (clone M1/70) from BioLegend; anti-mouse CCR3 (clone FAB729P) and anti-mouse CCR10 (clone FAB2815A) from R&D Systems. After staining, cells were fixed for 20 min with 4% paraformaldehyde (Fixation buffer; BioLegend). When intracellular staining was performed, cells were permeabilized (Permeabilization buffer; BioLegend), and the staining was performed in the same buffer following the manufacturer's instructions. Cells were analyzed on an LSRII flow cytometer (BD Biosciences) and the collected data were analyzed with FlowJo v10 software (TreeStar). For analysis of human neutrophils, whole-blood samples were collected in ethylenediaminetetraacetic acid (EDTA) for cellular analyses. Whole blood cell staining was performed using an Fc receptor blocking solution (Human TruStain FcX; BioLegend), the viability dye eFluor780 (Thermo Fisher), and the following conjugated monoclonal antibodies: PerCP/Cy5.5 anti-human CD45 antibody (clone HI30), Pacific Blue anti-mouse/human CD11b antibody (clone M1/70), FITC anti-human CD62L antibody (clone DREG-56), from BioLegend; PE anti-human CCR3 antibody (clone 61828), and APC anti-human CCR10 antibody (clone 314305) from R&D Systems. Samples were analyzed by flow cytometry using an LSR Fortessa flow cytometer (BD Biosciences), and data was analyzed using FlowJo v10 software.

In vitro neutrophil stimulation

Neutrophils were obtained from the bone marrow of C57/BL6 wild-type mice using the EasySep Mouse Enrichment Kit (STEMCELL), following the manufacturer's instructions. After enrichment, $1x10^6$ neutrophils were seeded in a round-bottom 96-well plate with RPMI media supplemented with 10% FBS, 1% antibiotic/antimycotic mix, and HEPES (1mM) (Invitrogen). For stimulation, cells were incubated with the following concentrations of recombinant mouse cytokines: TNFα (100 ng/mL), IFNγ (500 U/mL) and GM-CSF (10 ng/mL), all from R&D systems. Recombinant cytokines were added alone or in combination. For indicated experiments, polystyrene beads

(Thermo Fisher) were added to neutrophils at a 1:1 ratio. Cells were incubated for 4 hours at 37 ºC and 5% CO_2. After incubation, cells were recovered by centrifugation, washed with PBS, and processed for flow cytometry as described above.

Chemotaxis assay

Enriched neutrophils from the bone marrow of wild-type mice were stimulated with a cocktail of mouse recombinant cytokines (TNFα, IFNγ, GM-CSF), as described above, to induce receptor expression. After stimulation, cells were washed twice with PBS, resuspended in RPMI media supplemented with 0.1% BSA (w/v) to a final concentration of $1x10^7$ cells/mL, and 100 µL of the cell suspension were placed in the upper compartment of a Transwell chamber (3.0 µm pore size; Corning Costar). 50 nM of recombinant mouse CCL28, CCL11 (R&D Systems), or CXCL1 (Peprotech) were placed into the lower compartment of a Transwell chamber. The Transwell plate was then incubated for 2h at 37 °C. The number of cells that migrated to the lower compartment was determined by flow cytometry. The neutrophil chemotaxis index was calculated by dividing the number of cells that migrated in the presence of a chemokine by the number of cells that migrated in control chambers without chemokine stimulation.

Neutrophil *in vitro* infection and bacterial killing assays

Bone marrow neutrophils were obtained from mice as described above. *Salmonella* and *A. baumannii* were grown as described in the respective mouse experiment sections. Bacteria were then opsonized with 20% normal mouse serum for 30min at 37 °C. After neutrophils were enriched, $1x10^6$ neutrophils were seeded in a round-bottom 96-well plate and bacteria were added at a multiplicity of infection (MOI)= 10. The plate was centrifuged to ensure interaction between cells and bacteria. For flow cytometry analysis, cells were incubated for 1h at 37 °C and 5% CO_2.

Then, cells were recovered by centrifugation, washed with PBS, and processed for flow cytometry as described above. For inhibition of phagocytosis, bone marrow neutrophils were pre-incubated with cytochalasin D (10 μM) in DMSO (0.1%), or DMSO (vehicle), for 30 min prior to infection with opsonized *S*. Typhimurium for 1h at an MOI=10. For killing assays, recombinant mouse CCL28 (50nM) (Wang et al., 2000) and CCL11 (25nM) (Shamri et al., 2012) (R&D systems) were added to neutrophils. When indicated, the CCR3 receptor antagonist SB328437 (Tocris Bioscience) was added at a final concentration of 10 μM (White et al., 2000). Neutrophils infected with STm were incubated for 2.5h and neutrophils infected with *A. baumannii* were incubated for 4.5h at 37 ºC and 5% CO_2. After incubation, 1:2 dilution was performed with PBS supplemented with 2% Triton X-100 and then serial dilution was performed and plated on LB agar to enumerate bacteria. To calculate the percentage of bacterial survival, we divided the number of bacteria recovered in the presence of neutrophils by the number of bacteria recovered from wells that contained no neutrophils, then multiplied by 100.

Growth of *Salmonella* in media supplemented with recombinant chemokines

Cultures of *S.* Typhimurium wild-type were grown overnight at 37°C in LB supplemented with 50 μg/mL of nalidixic acid (Nal). The following day, cultures were diluted 1:100 in LB and grown at 37°C for 3 hr, subsequently diluted to ~0.5 x 10^6 CFU/mL in 1 mM potassium phosphate buffer (pH 7.2), then incubated at 37°C in the presence or absence of recombinant murine CCL28 (BioLegend) at the indicated concentrations. After 2h, samples were plated onto LB + Nal agar to enumerate viable bacteria. In other assays, *Salmonella* was grown as described above and ~1x10^7 CFU/mL were incubated at 37°C for 2.5h in the presence or absence of recombinant murine CCL28 (50 nM) (Wang et al., 2000) or CCL11 (25 nM) (Shamri et al., 2012) in RPMI medium supplemented with 10% FBS. After incubation, samples were plated onto LB + Nal agar to enumerate viable bacteria.

598

599 **RNA extraction and qPCR**

600 Total RNA was extracted from mouse cecal or lung tissue using Tri-Reagent (Molecular Research
601 Center). Reverse transcription of 1 µg of total RNA was performed using the SuperScript VILO
602 cDNA Synthesis kit (Thermo Fisher Scientific). Quantitative real-time PCR (qRT-PCR) for the
603 expression of *Actb* (β-actin), *Cxcl1, Tnfa, Ifng, Csf2, Il1b,* and *Il17a* was performed using the
604 PowerUp SYBR Green Master Mix (Applied Biosystems) on a QuantStudio 5 Real-Time PCR
605 System (Thermo Fisher Scientific). Gene expression was normalized to *Actb* (β-actin). Fold
606 changes in gene expression were relative to uninfected controls and calculated using the *ΔΔ*Ct
607 method.

608

609 **Histopathology**

610 Cecal and lung tissue samples were fixed in 10% buffered formalin, embedded in paraffin
611 according to standard procedures, and sectioned at 5 µm. Pathology scores of cecal and lung
612 samples were determined by blinded examinations of hematoxylin and eosin (H&E)-stained
613 sections. Each cecal section was evaluated using a semiquantitative score as described
614 previously (Moschen et al., 2016). Lung inflammation was assessed by a multiparametric scoring
615 based on previous work (Lammers et al., 2012).

616

617 **Immunofluorescence**

618 Deparaffinized lung sections were stained with a purified rat anti-mouse Ly6G antibody (clone
619 1A8, BioLegend) according to standard immunohistochemical procedures. Ly6G+ cells were
620 visualized by a goat anti-rat secondary antibody (Invitrogen). Cell nuclei were stained with DAPI

in SlowFade Gold Antifade Mountant (Invitrogen). Slides were scanned on a Zeiss Axio Scan.Z1 slide scanner and whole lung scans were evaluated with QuPath analysis software (Bankhead et al., 2017). Ly6G+ cells per mouse were quantified by averaging the neutrophil numbers of 3 consecutive high-power fields in regions with moderate to severe inflammation.

Statistical analysis

All statistical analysis was conducted in GraphPad Prism 8. Statistical significance was determined by using one-way ANOVA (multiple comparisons) or *t* test (single comparisons) for the *in vitro* experiments, or Mann-Whitney U for the *in vivo* experiments. Differences were considered statistically significant if the *p* value was <0.05.

Acknowledgements

This work was supported by the NIH (Public Health Service Grants AI121928) to MR, by a pilot project award from the NIAID Mucosal Immunology Studies Team (MIST) to APL, and by a grant from the InnovaUNAM of the National Autonomous University of Mexico (UNAM) and Alianza UCMX of the University of California, to APL and MR. RRG was partly supported by a fellowship from the Max Kade Foundation and by a fellowship from the Crohn's and Colitis Foundation. MHL was partly supported by NIH training grant T32 DK007202. ND was supported by NIH training grant NIH 5T32HD087978-05 and NIH NIAID grant 1-U01-AI124316. MR and VN are supported by Public Health Service Grant AI145325. Work in JLM-M lab was supported by CONACyT-FOSISS grant A3-S-36875 and UNAM-DGAPA-PAPIIT Program grant IN213020. Work in MR lab is also supported by Public Health Service Grants AI126277, AI145325, and AI154644, by the Chiba University-UCSD Center for Mucosal Immunology, Allergy, and Vaccines. MR holds an Investigator in the Pathogenesis of Infectious Disease Award from the Burroughs Wellcome Fund.

We would like to thank Dr. Albert Zlotnik for his thoughtful suggestions on the project over the years.

Author contributions

APL and MR conceived the overall study. APL, ND, SLB, RRG, MHL, S-PN, VN, and MR designed the *in vitro* and *in vivo* experiments and analyzed the data. APL, SS, ND, SLB, RRG, MHL, and KM performed experiments. APL, JT-R, VAS-H, RC-D, AP-F, SR-R, DG-M, and JLM-M performed the human neutrophil studies. RRG analyzed the histopathology. APL, S-PN, VN, and MR wrote the paper. APL, S-PN, VN, and MR provided supervision and funding support.

References

Ahuja, S.K., and Murphy, P.M. (1996). The CXC Chemokines Growth-regulated Oncogene (GRO) α, GROβ, GROγ, Neutrophil-activating Peptide-2, and Epithelial Cell-derived Neutrophil-activating Peptide-78 Are Potent Agonists for the Type B, but Not the Type A, Human Interleukin-8 Receptor. Journal of Biological Chemistry *271*, 20545–20550.

Ayoub Moubareck, C., and Hammoudi Halat, D. (2020). Insights into Acinetobacter baumannii: A Review of Microbiological, Virulence, and Resistance Traits in a Threatening Nosocomial Pathogen. Antibiotics (Basel) *9*.

Bankhead, P., Loughrey, M.B., Fernández, J.A., Dombrowski, Y., McArt, D.G., Dunne, P.D., McQuaid, S., Gray, R.T., Murray, L.J., Coleman, H.G., et al. (2017). QuPath: Open source software for digital pathology image analysis. Sci. Rep. *7*, 16878.

Barthel, M., Hapfelmeier, S., Quintanilla-Martínez, L., Kremer, M., Rohde, M., Hogardt, M., Pfeffer, K., Rüssmann, H., and Hardt, W.-D. (2003). Pretreatment of mice with streptomycin provides a Salmonella enterica serovar Typhimurium colitis model that allows analysis of both pathogen and host. Infect. Immun. *71*, 2839–2858.

Berger, M., Wetzler, E.M., Welter, E., Turner, J.R., and Tartakoff, A.M. (1991). Intracellular sites for storage and recycling of C3b receptors in human neutrophils. Proc. Natl. Acad. Sci. U. S. A. *88*, 3019–3023.

Bhatti, F.N., Burney, I.A., Moid, M.I., and Siddiqui, T. (1998). Bacterial isolates from neutropenic febrile pediatric patients and their sensitivity patterns to antibiotics. J. Pak. Med. Assoc. *48*, 287–290.

Burkhardt, A.M., Perez-Lopez, A., Ushach, I., Catalan-Dibene, J., Nuccio, S.-P., Chung, L.K., Hernandez-Ruiz, M., Carnevale, C., Raffatellu, M., and Zlotnik, A. (2019). CCL28 Is Involved in Mucosal IgA Responses, Olfaction, and Resistance to Enteric Infections. J. Interferon Cytokine Res. *39*, 214–223.

Capucetti, A., Albano, F., and Bonecchi, R. (2020). Multiple Roles for Chemokines in Neutrophil Biology. Front. Immunol. *11*, 1259.

Charo, I.F., and Ransohoff, R.M. (2006). The many roles of chemokines and chemokine receptors in inflammation. N. Engl. J. Med. *354*, 610–621.

Conroy, D.M., and Williams, T.J. (2001). Eotaxin and the attraction of eosinophils to the asthmatic lung. Respir. Res. *2*, 150–156.

Craig, A., Mai, J., Cai, S., and Jeyaseelan, S. (2009). Neutrophil recruitment to the lungs during bacterial pneumonia. Infect. Immun. *77*, 568–575.

Dillon, N., Holland, M., Tsunemoto, H., Hancock, B., Cornax, I., Pogliano, J., Sakoulas, G., and Nizet, V. (2019). Surprising synergy of dual translation inhibition vs. Acinetobacter baumannii and other multidrug-resistant bacterial pathogens. EBioMedicine *46*, 193–201.

English, K., Brady, C., Corcoran, P., Cassidy, J.P., and Mahon, B.P. (2006). Inflammation of the respiratory tract is associated with CCL28 and CCR10 expression in a murine model of allergic

asthma. Immunol. Lett. *103*, 92–100.

Fierer, J. (2001). Polymorphonuclear leukocytes and innate immunity to Salmonella infections in mice. Microbes Infect. *3*, 1233–1237.

Fu, J., Kong, J., Wang, W., Wu, M., Yao, L., Wang, Z., Jin, J., Wu, D., and Yu, X. (2020). The clinical implication of dynamic neutrophil to lymphocyte ratio and D-dimer in COVID-19: A retrospective study in Suzhou China. Thromb. Res. *192*, 3–8.

García-Patiño, M.G., García-Contreras, R., and Licona-Limón, P. (2017). The Immune Response against Acinetobacter baumannii, an Emerging Pathogen in Nosocomial Infections. Frontiers in Immunology *8*.

Garcia-Zepeda, E.A., Rothenberg, M.E., Ownbey, R.T., Celestin, J., Leder, P., and Luster, A.D. (1996). Human eotaxin is a specific chemoattractant for eosinophil cells and provides a new mechanism to explain tissue eosinophilia. Nat. Med. *2*, 449–456.

Grguric-Smith, L.M., Lee, H.H., Gandhi, J.A., Brennan, M.B., DeLeon-Rodriguez, C.M., Coelho, C., Han, G., and Martinez, L.R. (2015). Neutropenia exacerbates infection by Acinetobacter baumannii clinical isolates in a murine wound model. Frontiers in Microbiology *6*.

Gruber, C.N., Patel, R.S., Trachtman, R., Lepow, L., Amanat, F., Krammer, F., Wilson, K.M., Onel, K., Geanon, D., Tuballes, K., et al. (2020). Mapping Systemic Inflammation and Antibody Responses in Multisystem Inflammatory Syndrome in Children (MIS-C). Cell.

Hansson, M., Hermansson, M., Svensson, H., Elfvin, A., Hansson, L.-E., Johnsson, E., Sjöling, A., and Quiding-Järbrink, M. (2008). CCL28 is increased in human Helicobacter pylori-induced gastritis and mediates recruitment of gastric immunoglobulin A-secreting cells. Infect. Immun. *76*, 3304–3311.

Hartl, D., Krauss-Etschmann, S., Koller, B., Hordijk, P.L., Kuijpers, T.W., Hoffmann, F., Hector, A., Eber, E., Marcos, V., Bittmann, I., et al. (2008). Infiltrated neutrophils acquire novel chemokine receptor expression and chemokine responsiveness in chronic inflammatory lung diseases. J. Immunol. *181*, 8053–8067.

Hernández-Ruiz, M., and Zlotnik, A. (2017). Mucosal Chemokines. J. Interferon Cytokine Res. *37*, 62–70.

Hieshima, K., Ohtani, H., Shibano, M., Izawa, D., Nakayama, T., Kawasaki, Y., Shiba, F., Shiota, M., Katou, F., Saito, T., et al. (2003). CCL28 has dual roles in mucosal immunity as a chemokine with broad-spectrum antimicrobial activity. J. Immunol. *170*, 1452–1461.

Höchstetter, R., Dobos, G., Kimmig, D., Dulkys, Y., Kapp, A., and Elsner, J. (2000). The CC chemokine receptor 3 CCR3 is functionally expressed on eosinophils but not on neutrophils. Eur. J. Immunol. *30*, 2759–2764.

Hughes, C.E., and Nibbs, R.J.B. (2018). A guide to chemokines and their receptors. FEBS J. *285*, 2944–2971.

John, A.E., Thomas, M.S., Berlin, A.A., and Lukacs, N.W. (2005). Temporal production of CCL28 corresponds to eosinophil accumulation and airway hyperreactivity in allergic airway inflammation. Am. J. Pathol. *166*, 345–353.

731 Kitaura, M., Nakajima, T., Imai, T., Harada, S., Combadiere, C., Tiffany, H.L., Murphy, P.M., and
732 Yoshie, O. (1996). Molecular cloning of human eotaxin, an eosinophil-selective CC chemokine,
733 and identification of a specific eosinophil eotaxin receptor, CC chemokine receptor 3. J. Biol.
734 Chem. *271*, 7725–7730.

735 Kobayashi, Y. (2008). The role of chemokines in neutrophil biology. Front. Biosci. *13*, 2400–
736 2407.

737 Kobayashi, S.D., Voyich, J.M., Buhl, C.L., Stahl, R.M., and DeLeo, F.R. (2002). Global changes
738 in gene expression by human polymorphonuclear leukocytes during receptor-mediated
739 phagocytosis: cell fate is regulated at the level of gene expression. Proc. Natl. Acad. Sci. U. S.
740 A. *99*, 6901–6906.

741 Lammers, A.J.J., de Porto, A.P.N.A., de Boer, O.J., Florquin, S., and van der Poll, T. (2012).
742 The role of TLR2 in the host response to pneumococcal pneumonia in absence of the spleen.
743 BMC Infect. Dis. *12*, 139.

744 Lee, D.S., Lee, K.L., Jeong, J.B., Shin, S., Kim, S.H., and Kim, J.W. (2020a). Expression of
745 Chemokine CCL28 in Ulcerative Colitis Patients. Gut Liver.

746 Lee, H.H., Aslanyan, L., Vidyasagar, A., Brennan, M.B., Tauber, M.S., Carrillo-Sepulveda, M.A.,
747 Dores, M.R., Rigel, N.W., and Martinez, L.R. (2020b). Depletion of Alveolar Macrophages
748 Increases Pulmonary Neutrophil Infiltration, Tissue Damage, and Sepsis in a Murine Model of
749 Acinetobacter baumannii Pneumonia. Infect. Immun. *88*.

750 Lin, L., Nonejuie, P., Munguia, J., Hollands, A., Olson, J., Dam, Q., Kumaraswamy, M., Rivera,
751 H., Jr, Corriden, R., Rohde, M., et al. (2015). Azithromycin Synergizes with Cationic
752 Antimicrobial Peptides to Exert Bactericidal and Therapeutic Activity Against Highly Multidrug-
753 Resistant Gram-Negative Bacterial Pathogens. EBioMedicine *2*, 690–698.

754 Liu, W., Tao, Z.-W., Wang, L., Yuan, M.-L., Liu, K., Zhou, L., Wei, S., Deng, Y., Liu, J., Liu, H.-
755 G., et al. (2020). Analysis of factors associated with disease outcomes in hospitalized patients
756 with 2019 novel coronavirus disease. Chin. Med. J. *133*, 1032–1038.

757 Marchelletta, R.R., Gareau, M.G., Okamoto, S., Guiney, D.G., Barrett, K.E., and Fierer, J.
758 (2015). Salmonella-induced Diarrhea Occurs in the Absence of IL-8 Receptor (CXCR2)-
759 Dependent Neutrophilic Inflammation. J. Infect. Dis. *212*, 128–136.

760 Marcos, V., Zhou, Z., Yildirim, A.Ö., Bohla, A., Hector, A., Vitkov, L., Wiedenbauer, E.-M.,
761 Krautgartner, W.D., Stoiber, W., Belohradsky, B.H., et al. (2010). CXCR2 mediates NADPH
762 oxidase–independent neutrophil extracellular trap formation in cystic fibrosis airway
763 inflammation. Nat. Med. *16*, 1018–1023.

764 Matsuo, K., Nagakubo, D., Yamamoto, S., Shigeta, A., Tomida, S., Fujita, M., Hirata, T.,
765 Tsunoda, I., Nakayama, T., and Yoshie, O. (2018). CCL28-Deficient Mice Have Reduced IgA
766 Antibody-Secreting Cells and an Altered Microbiota in the Colon. J. Immunol. *200*, 800–809.

767 Mohan, T., Deng, L., and Wang, B.-Z. (2017). CCL28 chemokine: An anchoring point bridging
768 innate and adaptive immunity. Int. Immunopharmacol. *51*, 165–170.

769 Moschen, A.R., Gerner, R.R., Wang, J., Klepsch, V., Adolph, T.E., Reider, S.J., Hackl, H.,
770 Pfister, A., Schilling, J., Moser, P.L., et al. (2016). Lipocalin 2 Protects from Inflammation and

771 Tumorigenesis Associated with Gut Microbiota Alterations. Cell Host Microbe *19*, 455–469.

772 Nomiyama, H., Osada, N., and Yoshie, O. (2013). Systematic classification of vertebrate
773 chemokines based on conserved synteny and evolutionary history. Genes Cells *18*, 1–16.

774 Nouailles, G., Dorhoi, A., Koch, M., Zerrahn, J., Weiner, J., 3rd, Faé, K.C., Arrey, F., Kuhlmann,
775 S., Bandermann, S., Loewe, D., et al. (2014). CXCL5-secreting pulmonary epithelial cells drive
776 destructive neutrophilic inflammation in tuberculosis. J. Clin. Invest. *124*, 1268–1282.

777 Ogawa, H., Iimura, M., Eckmann, L., and Kagnoff, M.F. (2004). Regulated production of the
778 chemokine CCL28 in human colon epithelium. Am. J. Physiol. Gastrointest. Liver Physiol. *287*,
779 G1062–G1069.

780 O'Gorman, M.T., Jatoi, N.A., Lane, S.J., and Mahon, B.P. (2005). IL-1beta and TNF-alpha
781 induce increased expression of CCL28 by airway epithelial cells via an NFkappaB-dependent
782 pathway. Cell. Immunol. *238*, 87–96.

783 Pan, J., Kunkel, E.J., Gosslar, U., Lazarus, N., Langdon, P., Broadwell, K., Vierra, M.A.,
784 Genovese, M.C., Butcher, E.C., and Soler, D. (2000). Cutting Edge: A Novel Chemokine Ligand
785 for CCR10 And CCR3 Expressed by Epithelial Cells in Mucosal Tissues. The Journal of
786 Immunology *165*, 2943–2949.

787 Perez-Lopez, A., Behnsen, J., Nuccio, S.-P., and Raffatellu, M. (2016). Mucosal immunity to
788 pathogenic intestinal bacteria. Nat. Rev. Immunol. *16*, 135–148.

789 Raffatellu, M., George, M.D., Akiyama, Y., Hornsby, M.J., Nuccio, S.-P., Paixao, T.A., Butler,
790 B.P., Chu, H., Santos, R.L., Berger, T., et al. (2009). Lipocalin-2 resistance confers an
791 advantage to Salmonella enterica serotype Typhimurium for growth and survival in the inflamed
792 intestine. Cell Host Microbe *5*, 476–486.

793 Rudd, J.M., Pulavendran, S., Ashar, H.K., Ritchey, J.W., Snider, T.A., Malayer, J.R., Marie, M.,
794 Chow, V.T.K., and Narasaraju, T. (2019). Neutrophils Induce a Novel Chemokine Receptors
795 Repertoire During Influenza Pneumonia. Front. Cell. Infect. Microbiol. *9*, 108.

796 Sabroe, I., Jones, E.C., Whyte, M.K.B., and Dower, S.K. (2005). Regulation of human neutrophil
797 chemokine receptor expression and function by activation of Toll-like receptors 2 and 4.
798 Immunology *115*, 90–98.

799 Shamri, R., Melo, R.C.N., Young, K.M., Bivas-Benita, M., Xenakis, J.J., Spencer, L.A., and
800 Weller, P.F. (2012). CCL11 elicits secretion of RNases from mouse eosinophils and their cell-
801 free granules. FASEB J. *26*, 2084–2093.

802 Spencer, L.A., Melo, R.C.N., Perez, S.A.C., Bafford, S.P., Dvorak, A.M., and Weller, P.F.
803 (2006). Cytokine receptor-mediated trafficking of preformed IL-4 in eosinophils identifies an
804 innate immune mechanism of cytokine secretion. Proc. Natl. Acad. Sci. U. S. A. *103*, 3333–
805 3338.

806 Stojiljkovic, I., Bäumler, A.J., and Heffron, F. (1995). Ethanolamine utilization in Salmonella
807 typhimurium: nucleotide sequence, protein expression, and mutational analysis of the cchA
808 cchB eutE eutJ eutG eutH gene cluster. J. Bacteriol. *177*, 1357–1366.

809 Tsuchiya, T., Nakao, N., Yamamoto, S., Hirai, Y., Miyamoto, K., and Tsujibo, H. (2012). NK1. 1+

cells regulate neutrophil migration in mice with Acinetobacter baumannii pneumonia. Microbiol. Immunol. *56*, 107–116.

Uribe-Querol, E., and Rosales, C. (2020). Phagocytosis: Our Current Understanding of a Universal Biological Process. Front. Immunol. *11*, 1066.

Van Faassen, H., KuoLee, R., Harris, G., Zhao, X., Conlan, J.W., and Chen, W. (2007). Neutrophils play an important role in host resistance to respiratory infection with Acinetobacter baumannii in mice. Infect. Immun. *75*, 5597–5608.

Vassiloyanakopoulos, A.P., Okamoto, S., and Fierer, J. (1998). The crucial role of polymorphonuclear leukocytes in resistance to Salmonella dublin infections in genetically susceptible and resistant mice. Proc. Natl. Acad. Sci. U. S. A. *95*, 7676–7681.

Veras, F.P., Pontelli, M.C., Silva, C.M., Toller-Kawahisa, J.E., de Lima, M., Nascimento, D.C., Schneider, A.H., Caetité, D., Tavares, L.A., Paiva, I.M., et al. (2020). SARS-CoV-2–triggered neutrophil extracellular traps mediate COVID-19 pathology. J. Exp. Med. *217*.

Wang, W., Soto, H., Oldham, E.R., Buchanan, M.E., Homey, B., Catron, D., Jenkins, N., Copeland, N.G., Gilbert, D.J., Nguyen, N., et al. (2000). Identification of a novel chemokine (CCL28), which binds CCR10 (GPR2). J. Biol. Chem. *275*, 22313–22323.

White, J.R., Lee, J.M., Dede, K., Imburgia, C.S., Jurewicz, A.J., Chan, G., Fornwald, J.A., Dhanak, D., Christmann, L.T., Darcy, M.G., et al. (2000). Identification of potent, selective non-peptide CC chemokine receptor-3 antagonist that inhibits eotaxin-, eotaxin-2-, and monocyte chemotactic protein-4-induced eosinophil migration. J. Biol. Chem. *275*, 36626–36631.

Yamada, K., Yanagihara, K., Kaku, N., Harada, Y., Migiyama, Y., Nagaoka, K., Morinaga, Y., Nakamura, S., Imamura, Y., Miyazaki, T., et al. (2013). Azithromycin attenuates lung inflammation in a mouse model of ventilator-associated pneumonia by multidrug-resistant Acinetobacter baumannii. Antimicrob. Agents Chemother. *57*, 3883–3888.

Yaman, Y., Devrim, İ., Ozek, G., Demirağ, B., Oymak, Y., Gülfidan, G., and Vergin, C. (2018). Non-typhoidal Salmonella bacteraemia in paediatric leukaemia patients. Contemp. Oncol. *22*, 105–107.

Yan Yan, Jiang, X., Wang, X., Liu, B., Ding, H., Jiang, M., Yang, Z., Dai, Y., Ding, D., Yu, H., et al. (2020). CCL28 mucosal expression in SARS-CoV-2-infected patients with diarrhea in relation to disease severity. J. Infect. 4822.

Zeng, X., Gu, H., Cheng, Y., Jia, K.-R., Liu, D., Yuan, Y., Chen, Z.-F., Peng, L.-S., Zou, Q.-M., and Shi, Y. (2019). A lethal pneumonia model of Acinetobacter baumannii: an investigation in immunocompetent mice. Clin. Microbiol. Infect. *25*, 516.e1–e516.e4.

Zeng, X., Gu, H., Peng, L., Yang, Y., Wang, N., Shi, Y., and Zou, Q. (2020). Transcriptome Profiling of Lung Innate Immune Responses Potentially Associated With the Pathogenesis of Acinetobacter baumannii Acute Lethal Pneumonia. Front. Immunol. *11*, 708.

Zlotnik, A., and Yoshie, O. (2000). Chemokines: a new classification system and their role in immunity. Immunity *12*, 121–127.

Zlotnik, A., Burkhardt, A.M., and Homey, B. (2011). Homeostatic chemokine receptors and

849 organ-specific metastasis. Nat. Rev. Immunol. *11*, 597–606.

850

851 **FIGURES AND LEGENDS**

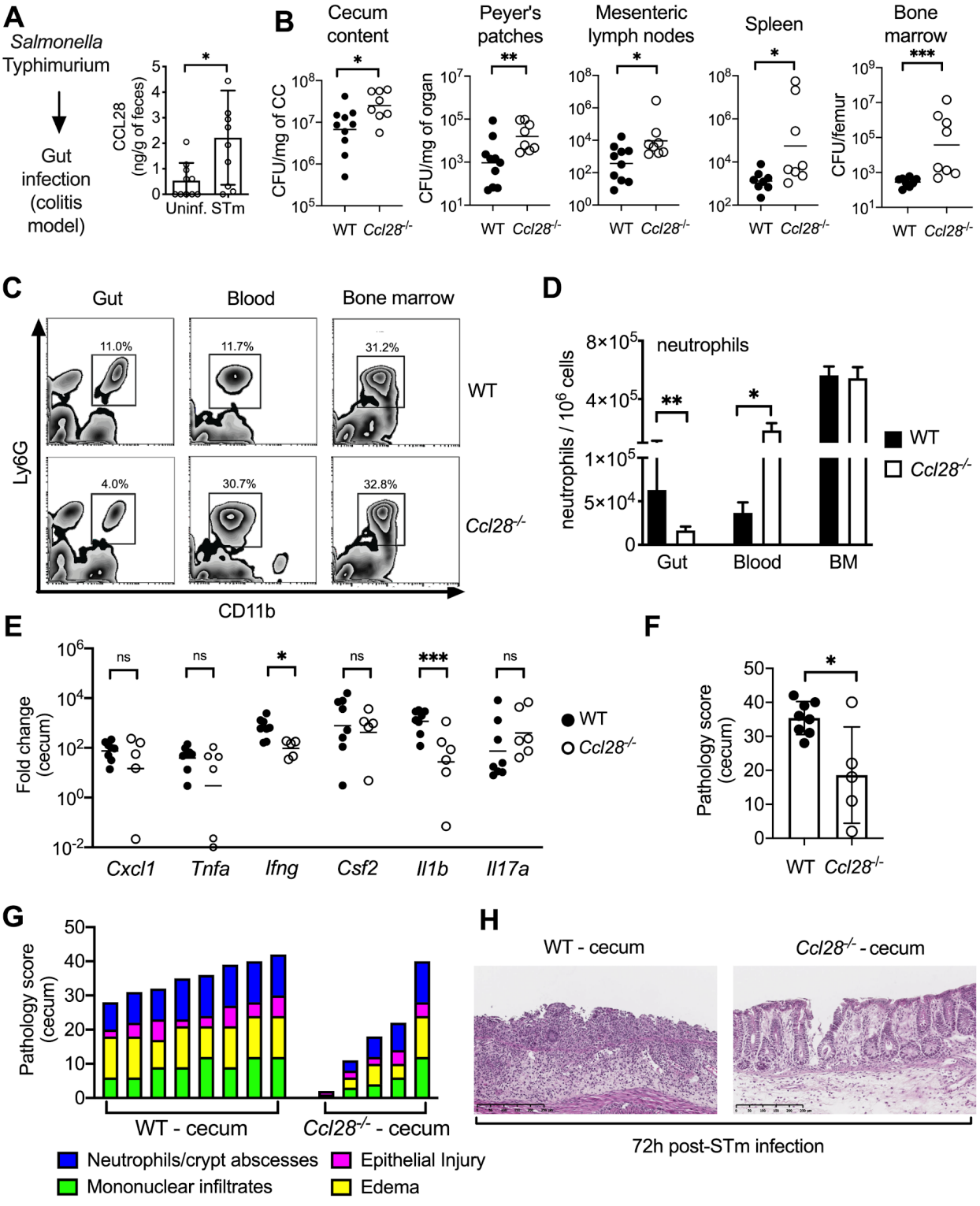

852 Figure 1

Figure 1. CCL28 confers protection during *Salmonella* colitis and mediates the recruitment of neutrophils to the gut. (**A**) For the colitis model, wild-type mice were gavaged with streptomycin 24h prior to oral infection with *S. enterica* serovar Typhimurium (STm). At 96h post-infection, CCL28 in feces was quantified by ELISA. Data shown comprise two independent experiments (uninfected, n=10; STm, n=10). Bars represent the mean ± SD. (**B**) CFU in cecum content, Peyer's patches, mesenteric lymph nodes, spleen, and bone marrow were determined at 72h post-infection of wild-type (WT, black circles) and *Ccl28*$^{-/-}$ (white circles) littermate mice. Data shown comprise three independent experiments (WT, n=10; *Ccl28*$^{-/-}$, n=8). Bars represent the geometric mean. (**C**) Representative contour plots of neutrophils (CD11b^{+} Ly6G^{+} cells; gated on live, CD45^{+} cells) obtained from the gut, blood, and bone marrow of STm-infected WT or *Ccl28*$^{-/-}$ mice, as determined by flow cytometry at 48h post-infection. (**D**) Frequency of neutrophils per million live cells obtained from the gut, blood, and bone marrow of STm-infected WT (black bars) or *Ccl28*$^{-/-}$ mice (white bars). Data shown comprise three independent experiments (WT, n=15; *Ccl28*$^{-/-}$, n=15). Bars represent the mean ± SD. (**E**) Relative expression levels (qPCR) of *Cxcl1* (CXCL1), *Tnfa* (TNFα), *Ifng* (IFNγ), *Csf2* (GM-CSF), *Il1b* (IL-1β), and *Il17a* (IL-17A) in the cecum of WT (black circles, n=8) or *Ccl28*$^{-/-}$ mice (white circles, n=6). Bars represent the geometric mean. Data shown comprise three independent experiments. (**F-H**) Histopathological analysis of cecum collected from STm-infected WT or *Ccl28*$^{-/-}$ mice (WT, n=8; *Ccl28*$^{-/-}$, n=5). (**F**) Sum of the total histopathology score, (**G**) histopathology scores showing the analyzed parameters, and (**H**) H&E-stained sections from one representative animal for each group (200X). (**F**) Bars represent the mean ± SD. A significant change (Mann-Whitney U) relative to WT controls is indicated by *$p \leq 0.05$, **$p \leq 0.01$, ***$p \leq 0.001$. ns = not significant.

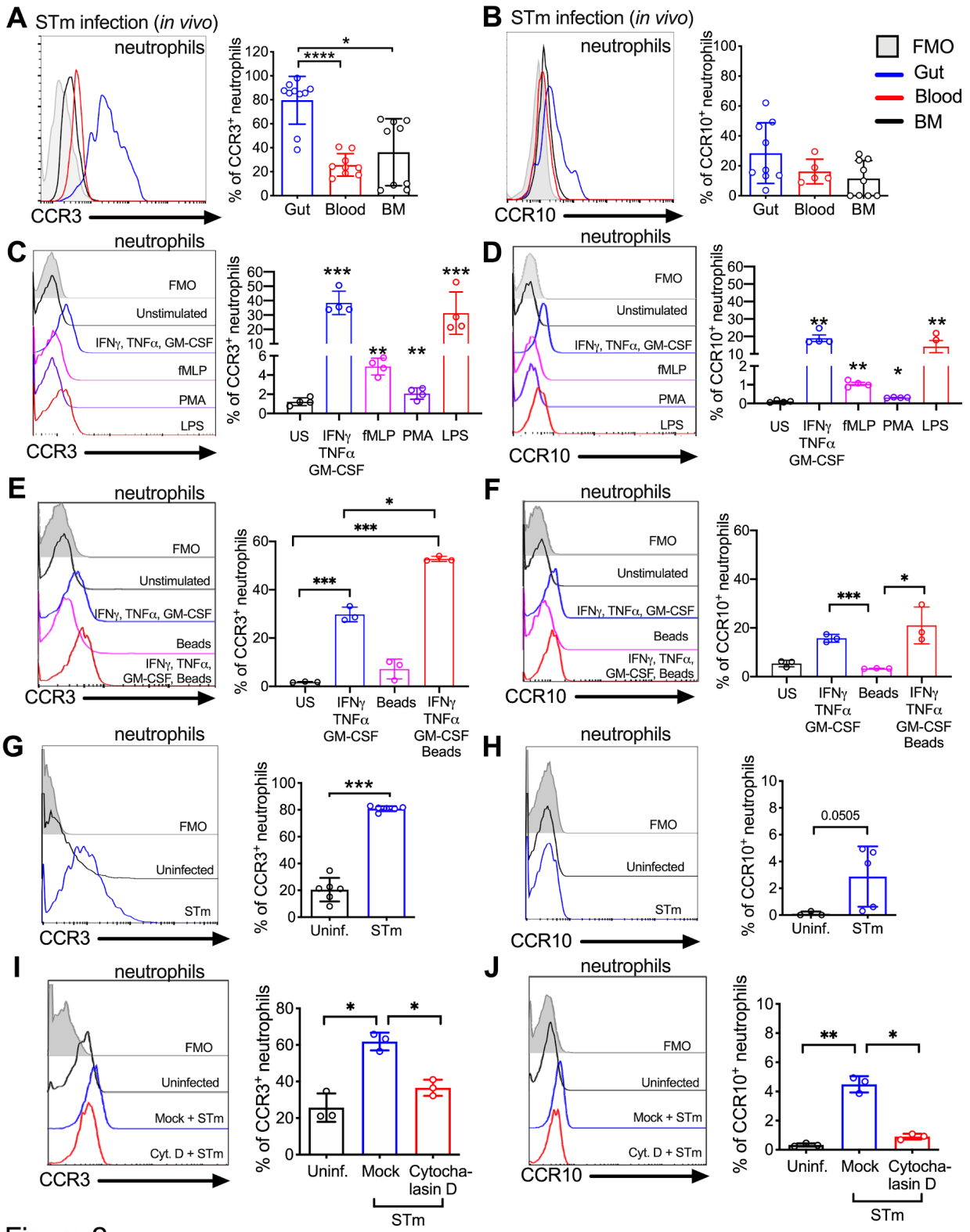

Figure 2

879 **Figure 2. Surface expression of the CCL28 receptors CCR3 and CCR10 on neutrophils**
880 **upon stimulation with proinflammatory stimuli and phagocytosis. (A-B)** Surface expression
881 of (**A**) CCR3 or (**B**) CCR10 on neutrophils obtained from the gut, blood, and bone marrow 72h
882 post-infection with STm, analyzed by flow cytometry. Left panels show representative histograms
883 of (**A**) CCR3 or (**B**) CCR10 expression on the surface of neutrophils (gated on live, $CD45^+$ $CD11b^+$
884 $Ly6G^+$ cells) from the gut (blue), blood (red), and bone marrow (BM; black). Right panels show
885 the percentage of (**A**) $CCR3^+$ or (**B**) $CCR10^+$ neutrophils obtained from gut, blood, and BM. Data
886 are from two independent experiments. (**C-F**) Bone marrow neutrophils were unstimulated or
887 treated with the indicated stimuli for 4h. Surface expression of (**C**, **E**) CCR3 and (**D**, **F**) CCR10 on
888 neutrophils was determined by flow cytometry. Left panels show representative histograms of (**C,**
889 **E**) CCR3 or (**D, F**) CCR10 surface expression after stimulation with: (**C, D**) cytokines TNFα + IFNγ
890 + GM-CSF (blue); fMLP (magenta); PMA, (purple); LPS (red); (**E, F**) cytokines TNFα + IFNγ +
891 GM-CSF (blue); beads alone (magenta); cytokines plus beads (red). Right panels show the
892 percentage of (**C, E**) $CCR3^+$ or (**D**, **F**) $CCR10^+$ neutrophils following stimulation with the indicated
893 stimuli. US = unstimulated. Data shown are representative of two independent experiments. (**G,**
894 **H**) Bone marrow neutrophils were infected with opsonized *S*. Typhimurium at a multiplicity of
895 infection (MOI)=10 for 1h. Surface expression of (**G**) CCR3 or (**H**) CCR10 was determined by flow
896 cytometry. Data are from two independent experiments. (**I, J**) Bone marrow neutrophils were
897 treated with cytochalasin D or mock-treated with DMSO (vehicle) for 30 min before infection with
898 opsonized STm for 1h at an MOI=10. Surface expression of (**I**) CCR3 or (**J**) CCR10 was
899 determined by flow cytometry. Data shown is representative of two independent experiments. Left
900 panels show representative histograms of surface receptor staining on neutrophils, and right
901 panels show the percentages. (**A-J**, right panels) Bars represent the mean ± SD. (**A**-**F**, **I**, **J**) Data
902 was analyzed by one-way ANOVA on log-transformed data. (**G, H**) Data was analyzed by paired
903 *t* test. Significant changes are indicated by $*p \leq 0.05$, $**p \leq 0.01$,$***p \leq 0.001$, $****p \leq 0.0001$.

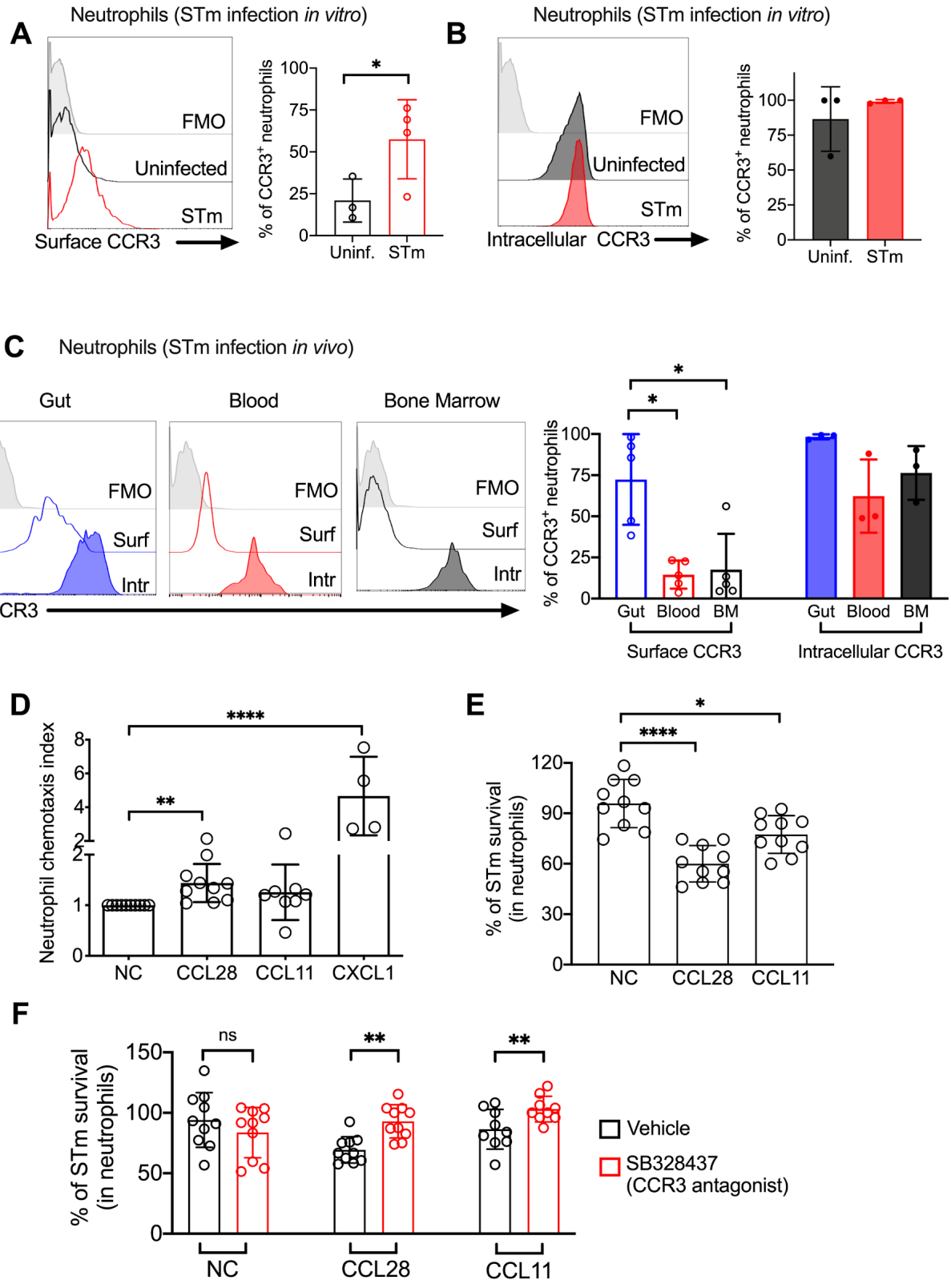

Figure 3

Figure 3. CCL28 modulates neutrophil chemotaxis and antimicrobial activity. (**A, B**) Bone marrow neutrophils were infected with opsonized STm at MOI=10 for 1h. (**A**) Surface CCR3 or (**B**) intracellular CCR3 were detected by flow cytometry. (**C**) Neutrophils were obtained from the gut, blood, and bone marrow 72h post-infection with STm. Surface (clear histograms) or intracellular (solid histograms) CCR3 expression was analyzed by flow cytometry. (**A-C**) Left panels show representative histograms, and right panels show the percentage of neutrophils expressing CCR3 on their surface (clear bars) or intracellularly (solid bars). (**D**) Bone marrow neutrophils were stimulated with TNFα + IFNγ + GM-CSF for 4h before adding $1x10^6$ cells to the upper compartment of a transwell chamber for chemotaxis assays. Each of the chemokines (CCL28, CCL11, or CXCL1), or no chemokine (NC), were placed in separate lower compartments. The transwell plate was incubated for 2h at 37ºC. Cells that migrated to the lower compartment were enumerated by flow cytometry. Neutrophil chemotaxis index was calculated by taking the number of cells that migrated in response to a chemokine and dividing it by the number of cells that migrated in the absence of a chemokine. Data are from four independent experiments. (**E**) Opsonized STm ($1x10^7$ CFU) was cultured alone, or added to bone marrow neutrophils ($1x10^6$ cells) stimulated with CCL28, CCL11, or no chemokine, for 2.5h at 37ºC. CFU were enumerated by plating serial dilutions. Percentage of STm survival was calculated for each condition by taking the CFU from bacteria incubated with neutrophils and dividing it by the CFU from bacteria incubated without neutrophils, multiplied by 100. Data shown comprise three independent experiments. (**F**) The effect of the CCR3 antagonist SB328437 on neutrophil-mediated STm killing was evaluated by performing the experiment as described in panel (**E**), with or without the antagonist. Data shown comprise three independent experiments. (**A**-**F**) Bars represent the mean ± SD. Data was analyzed by one-way ANOVA on log-transformed data. (**F**) Data was analyzed by paired *t* test. Significant changes are indicated by $*p \leq 0.05$, $**p \leq 0.01$, $****p \leq 0.0001$. ns = not significant.

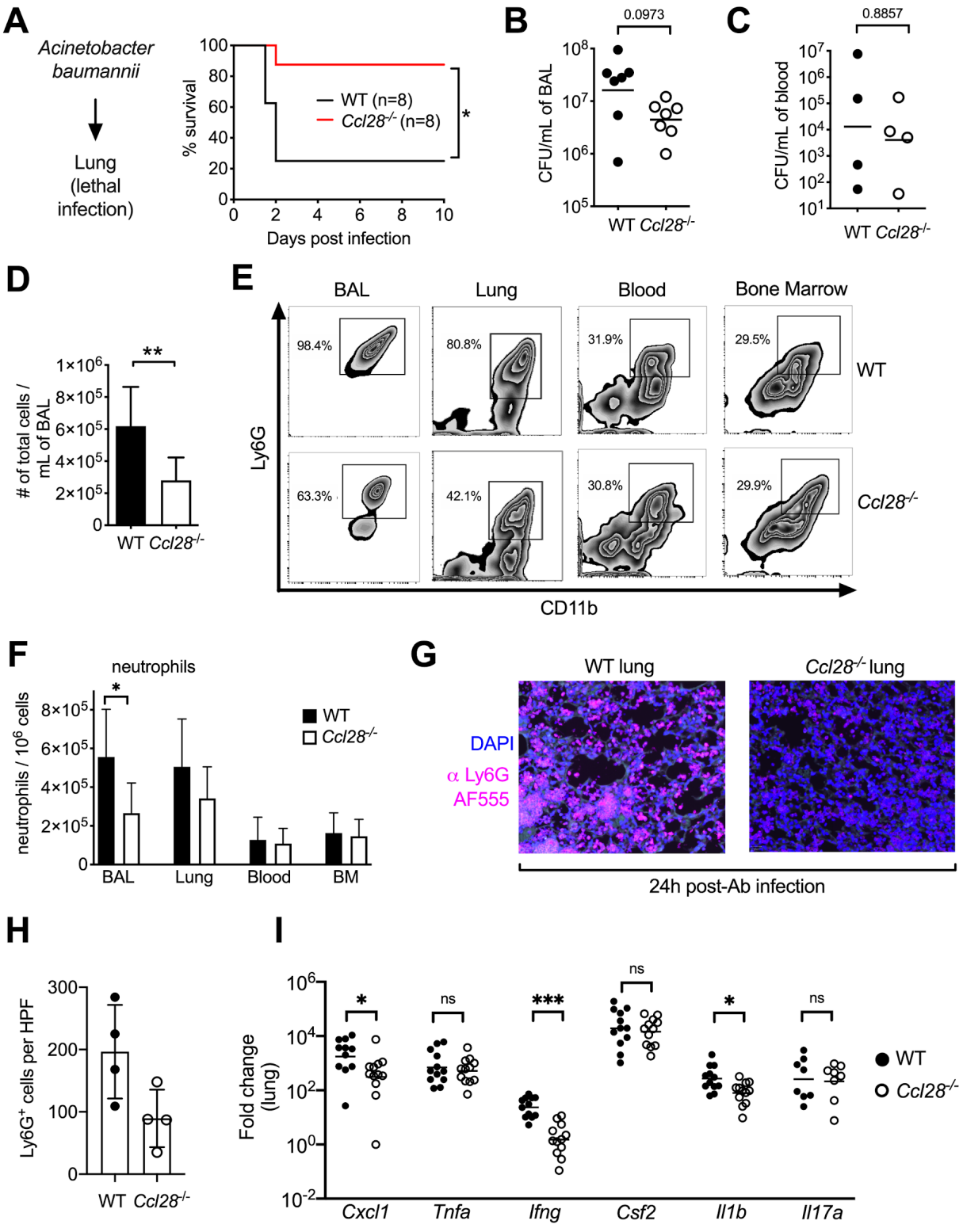

Figure 4

Figure 4. Absence of CCL28 confers protection in a lethal *Acinetobacter* pneumonia model. (**A**) WT mice (black line) and *Ccl28*$^{-/-}$ mice (red line) were intratracheally infected with *Acinetobacter baumannii* (Ab) and their survival was determined for 10 days. Data shown comprise two independent experiments (WT, n=8; *Ccl28*$^{-/-}$, n=8). (**B-F**) WT and *Ccl28*$^{-/-}$ mice were compared 24h post-infection with Ab. (**B, C**) Ab CFU in (**B**) BAL (bronchoalveolar lavage) fluid or (**C**) blood in WT mice (black circles) and *Ccl28*$^{-/-}$ mice (white circles). (**D**) The number of total host cells per mL of BAL, as determined by flow cytometry. (**E, F**) Representative (**E**) contour plots of neutrophils (CD11b^{+} Ly6G^{+} cells; gated on live, CD45^{+} cells) and (**F**) frequency of neutrophils obtained from the BAL, lung, blood, and bone marrow of Ab-infected WT or *Ccl28*$^{-/-}$ mice, as determined by flow cytometry. Data comprise two independent experiments (WT, n=8; *Ccl28*$^{-/-}$, n=8). Bars represent (**B, C**) the geometric mean or (**D, F**) the mean ± SD. (**G**) Representative immunofluorescence image showing Ly6G^{+} cells (magenta) in the lungs of WT and *Ccl28*$^{-/-}$ mice 24h post-Ab infection. DAPI (blue) was used to label nuclei. (**H**) Quantification of Ly6G^{+} cells per high-power field (HPF) from immunofluorescence images of lungs from WT mice (n=4) and *Ccl28*$^{-/-}$ mice (n=4). Bars represent the mean ± SD. (**I**) Relative expression levels (qPCR) of *Cxcl1* (CXCL1), *Tnfa* (TNFα), *Ifng* (IFNγ), *Csf2* (GM-CSF), *Il1b* (IL-1β), and *Il17a* (IL-17A) in the lung of WT (black circles, n=12) or *Ccl28*$^{-/-}$ mice (white circles, n=12) infected with Ab. Bars represent the geometric mean. Data shown comprise three independent experiments. A significant change (Mann-Whitney U) relative to WT controls is indicated by *$p \leq 0.05$, **$p \leq 0.01$, ***$p \leq 0.001$. ns = not significant.

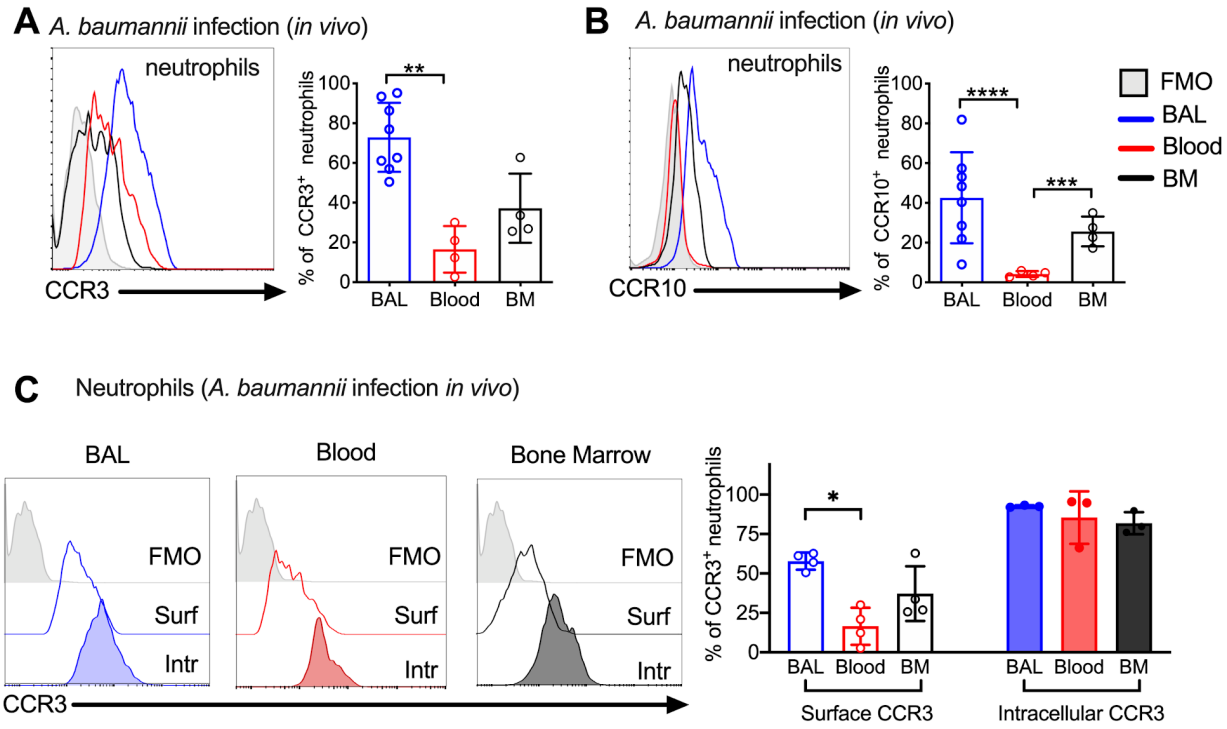

Figure 5

Figure 5. Lung neutrophils express CCR3 and CCR10 in an *Acinetobacter* lethal pneumonia model. WT mice were infected with *A. baumannii* (Ab) for 24h. (**A-C**) Cells obtained from BAL, blood, and bone marrow were analyzed by flow cytometry to determine: (**A**) CCR3 or (**B**) CCR10 surface expression on neutrophils ($CD11b^+$ $Ly6G^+$ cells; gated on live, $CD45^+$ cells); (**C**) Surface (clear histograms) or intracellular (solid histograms) CCR3 expression in neutrophils. Data shown comprise two independent experiments. (**A-C**) Left panels show representative histograms, and right panels show the percentage of neutrophils expressing the indicated receptor on their surface (clear bars) or intracellularly (solid bars). (**D**) Bone marrow neutrophils were infected with opsonized Ab at an MOI=10 for 1h. Surface CCR3 was determined by flow cytometry. Left panel shows representative histograms of CCR3 expression, and the right panel shows the percentage of $CCR3^+$ neutrophils. Data are from two independent experiments. (**E**) Opsonized Ab ($1x10^7$ CFU) was cultured alone, or added to bone marrow neutrophils ($1x10^6$ cells) stimulated with CCL28, CCL11, or no chemokine (NC), for 4.5h at 37°C. CFU were enumerated by plating serial dilutions. Percentage of Ab survival was calculated for each condition by taking the CFU from bacteria incubated with neutrophils and dividing it by the CFU from bacteria incubated without neutrophils, multiplied by 100. Data shown comprise three independent experiments. Bars represent the mean ± SD. (**A-C**, **E**) Data was analyzed by one-way ANOVA on log-transformed data. (**D**) Data was analyzed by paired *t* test. Significant changes are indicated by $*p \leq 0.05$, $**p \leq 0.01$, $***p \leq 0.001$, $****p \leq 0.0001$.

979 **SUPPLEMENTAL FIGURES**

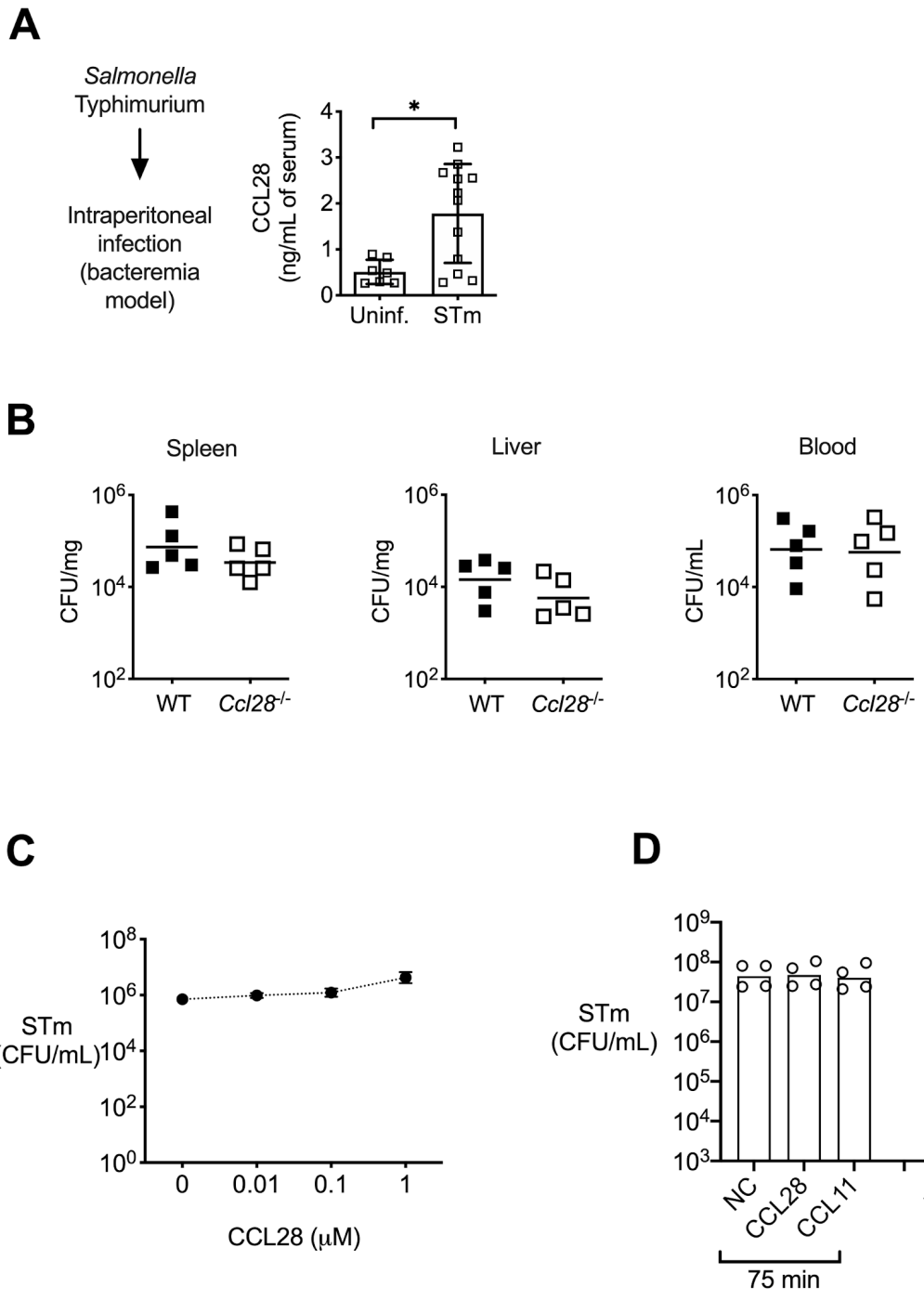

980 Supp. Fig. 1

Supplementary Figure 1. CCL28 does not confer protection in a *Salmonella* bacteremia model, and lacks direct antimicrobial activity against *Salmonella*.

(**A, B**) For the bacteremia model, mice were infected by intraperitoneal injection with *S.* Typhimurium (STm, $1x10^3$ CFU) or sterile PBS (uninfected control). (**A**) At 96h post-infection, CCL28 in serum was quantified by ELISA of wild-type mice (uninfected, n=7; STm, n=12). Data shown comprise two independent experiments. Bars represent the mean ± SD. (**B**) STm CFU was determined in the spleen, liver, and blood of WT mice (black squares) and *Ccl28*$^{-/-}$ mice (white squares) 96h after intraperitoneal infection with STm ($1x10^3$ CFU). Data shown comprise two independent experiments (WT, n=5; *Ccl28*$^{-/-}$, n=5). (**C, D**) *In vitro* antimicrobial activity of CCL28 against STm. (**C**) STm ($0.5x10^6$ CFU/mL) was incubated with recombinant murine CCL28 at the indicated concentrations (n=6 per group) and CFU were enumerated after 2h. (**D**) STm ($1x10^7$ CFU/mL) was incubated with recombinant murine CCL28 (50 nM) or CCL11 (25 nM) and CFU were enumerated at 75 min (n=4 per group) and 150 min (n=6 per group). Bars represent the geometric mean. A significant change (Mann-Whitney U) relative to uninfected controls is indicated by $*p \leq 0.05$.

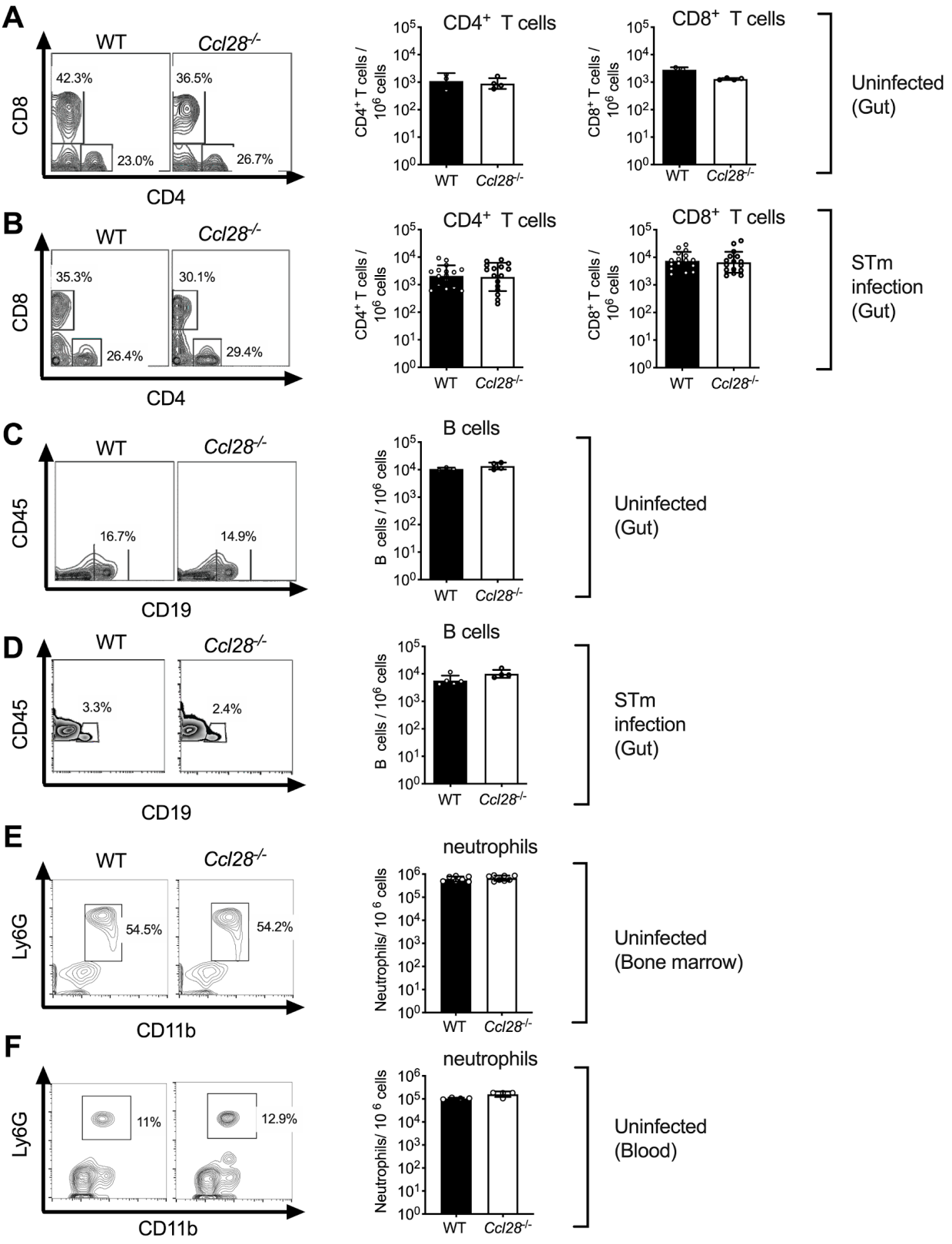

Supp. Fig. 2

Supplementary Figure 2. **Wild-type and *Ccl28*$^{-/-}$ mice exhibit similar numbers of T and B cells, as well as bone marrow and blood neutrophils.**

Flow cytometry analysis of (**A**, **B**) CD4^{+} and CD8^{+} T cells, and (**C**, **D**) CD19^{+} B cells isolated from the gut of (**A, C**) uninfected WT and *Ccl28*$^{-/-}$ mice or (**B, D**) WT and *Ccl28*$^{-/-}$ mice infected with STm for 48h (colitis model; see also **Fig. 1**). (**E, F**) Cells from (**E**) bone marrow or (**F**) blood of uninfected WT (black bars) or *Ccl28*$^{-/-}$ (white bars) mice were analyzed by flow cytometry to determine the percentage and number of neutrophils. (**A-F**) Left panels show representative contour plots. Right panels show the frequency of the indicated cells per million live cells of WT mice (black bars) and *Ccl28*$^{-/-}$ mice (white bars). Each circle represents a mouse. Bars represent the geomean ± SD.

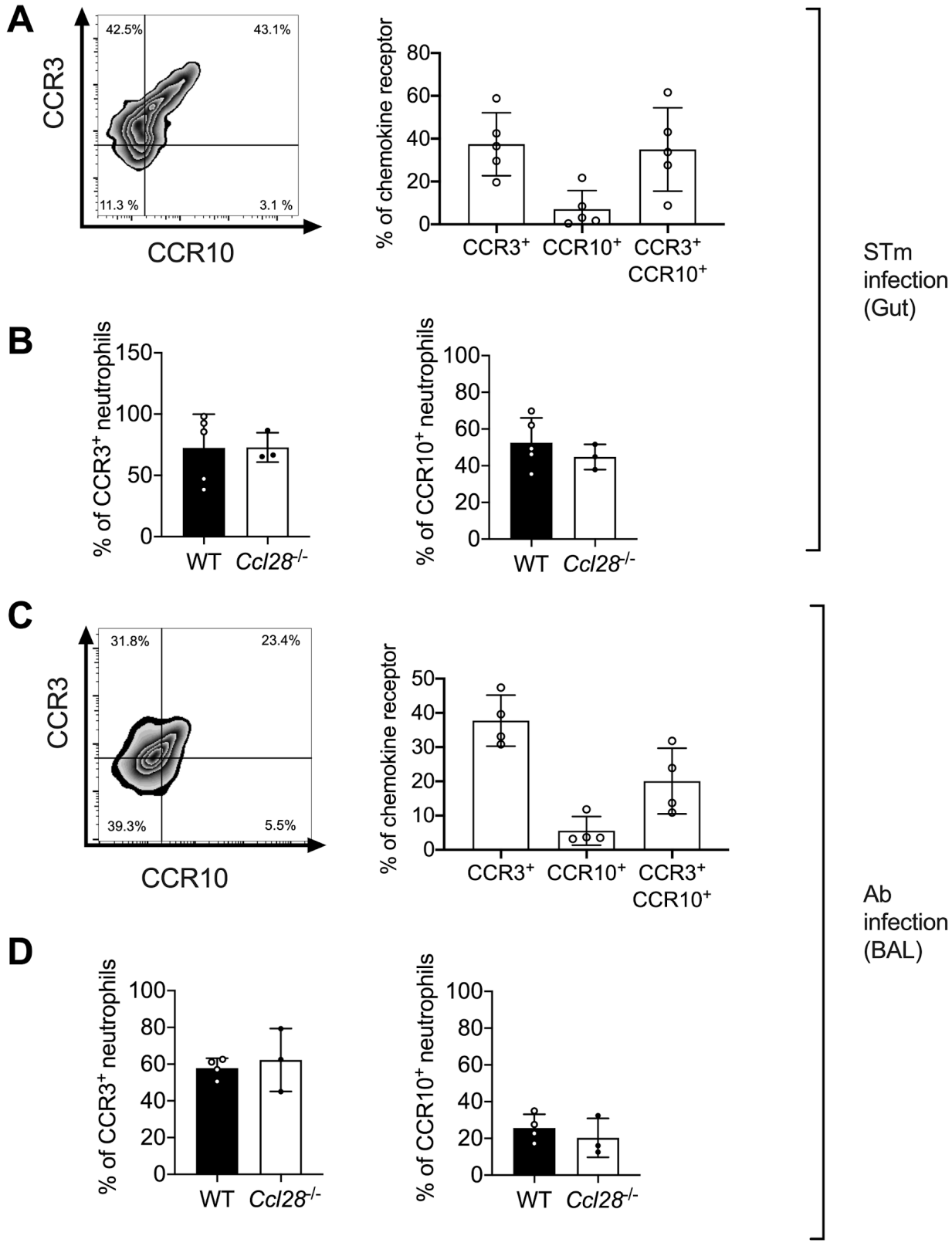

Supp. Fig. 3

Supplementary Figure 3. **Expression of CCR3 and CCR10 in neutrophils isolated from the gut and lung mucosa.**

(**A**) Surface expression of CCR3 and CCR10 on neutrophils obtained from the gut of WT mice (n=5) infected with STm for 72h, analyzed by flow cytometry. (**B**) Percentage of $CCR3^+$ and $CCR10^+$ neutrophils obtained from the gut of WT (n=5) and *Ccl28*$^{-/-}$ mice (n=3) infected with STm for 72h, analyzed by flow cytometry. (**C**) Surface expression of CCR3 and CCR10 on neutrophils obtained from the BAL of WT mice (n=4) infected with Ab for 24h, analyzed by flow cytometry. (**D**) Percentage of $CCR3^+$ and $CCR10^+$ neutrophils obtained from the BAL of WT (n=4) and *Ccl28*$^{-/-}$ mice (n=3) infected with Ab for 24h, analyzed by flow cytometry. (**A**, **C**) Left panels show representative contour plots, and right panels show the percentages of neutrophils expressing the indicated receptor on their surface. Bars represent the mean ± SD.

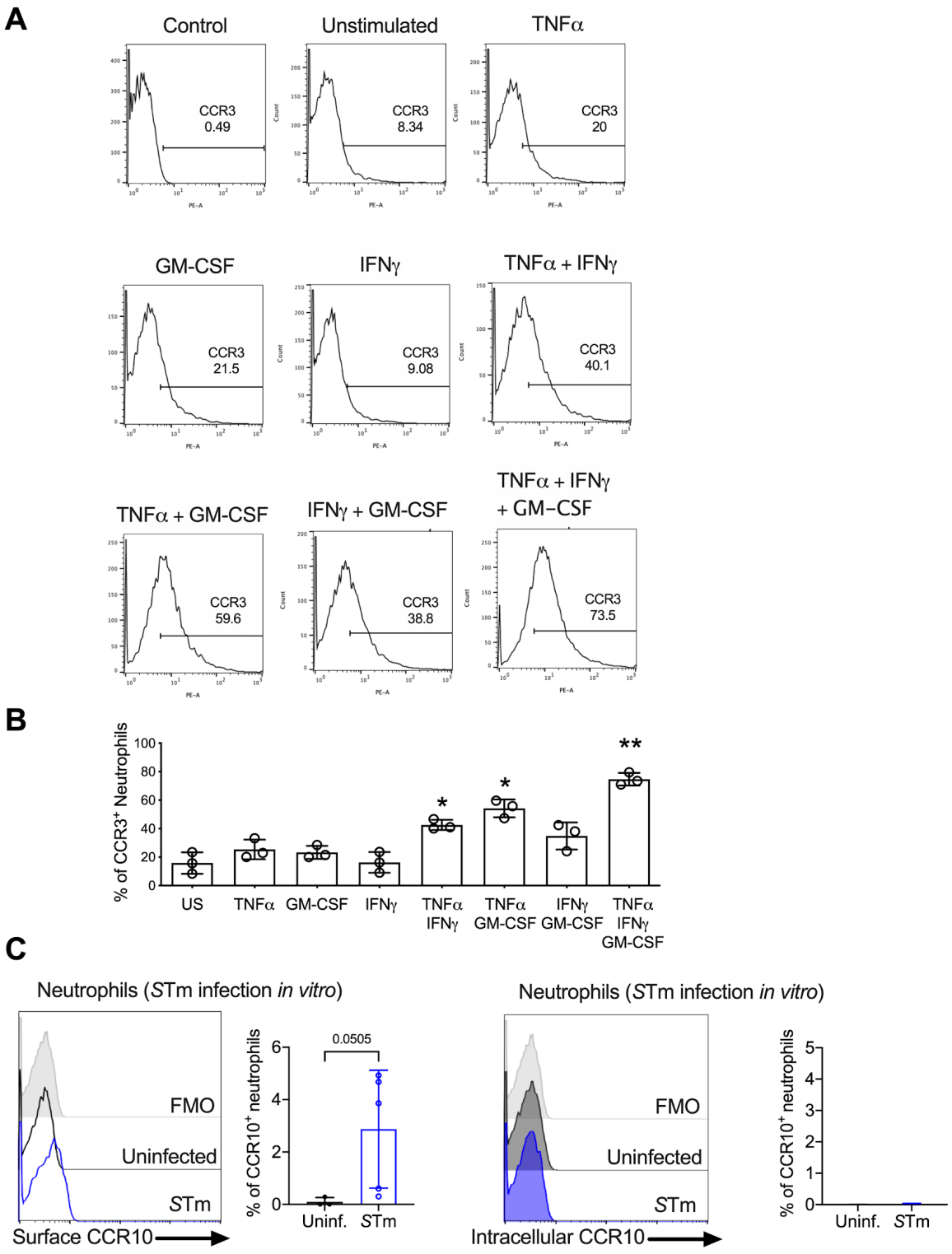

Supp. Fig. 4

Supplementary Figure 4. CCR3 surface expression is enhanced in bone marrow neutrophils stimulated with a cytokine cocktail.

Bone marrow neutrophils were incubated with the indicated cytokines for 4h, and surface expression of CCR3 was evaluated by flow cytometry. (**A**) Representative histograms and (**B**) percentage of $CCR3^+$ neutrophils. Bars represent the mean ± SD. Data shown are representative of two independent experiments, and statistical analysis was performed by a paired *t* test. Significant changes are indicated by $*p \leq 0.05$, $**p \leq 0.01$. (**C**) Bone marrow neutrophils were infected with opsonized *S*Tm at MOI=10 for 1h. Surface (left panels) or intracellular (right panels) CCR10 was detected by flow cytometry. Surface CCR10 is also shown in **Fig. 2H** and displayed here for comparison.

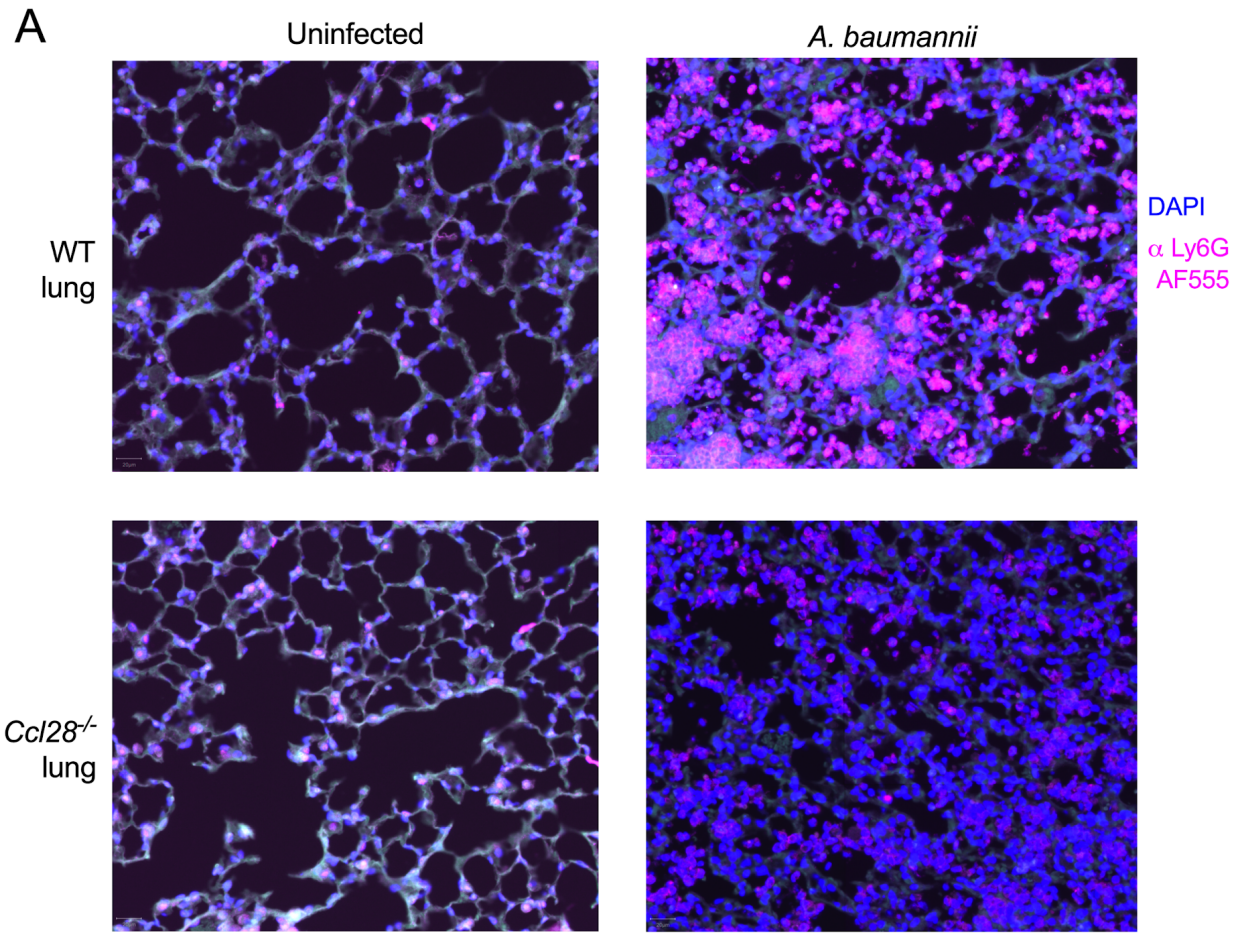

Supp. Fig. 5

1037

Supplementary Figure 5. Immunofluorescence staining and histopathology of *Acinetobacter*-infected lungs from WT and *Ccl28*$^{-/-}$ mice.

(**A**) Representative immunofluorescence image of lungs from WT and *Ccl28*$^{-/-}$ mice, uninfected or infected with *A. baumannii* (Ab) stained for the neutrophil marker Ly6G (magenta). DAPI (blue) was used to label nuclei. (**B**) Quantification of Ly6G^{+} cells in lungs from WT and *Ccl28*$^{-/-}$ mice, uninfected or infected with Ab. Bars represent the mean ± SD, and each circle represents an individual mouse. (**C**) Histopathological analysis of lungs from WT and *Ccl28*$^{-/-}$ mice infected with Ab at 24 h post-infection. Each bar represents an individual mouse

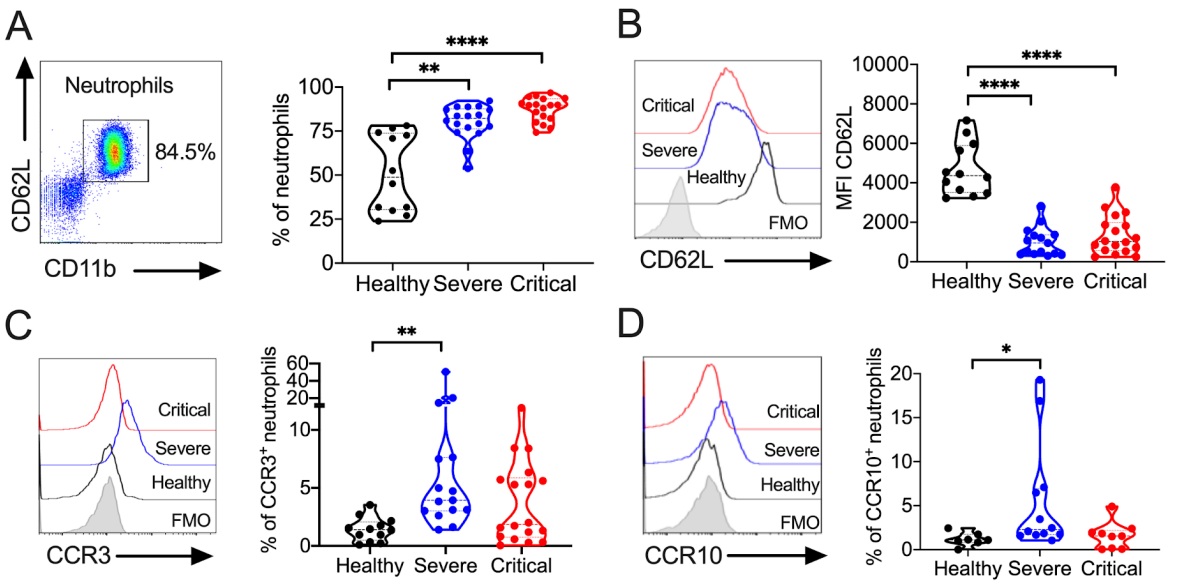

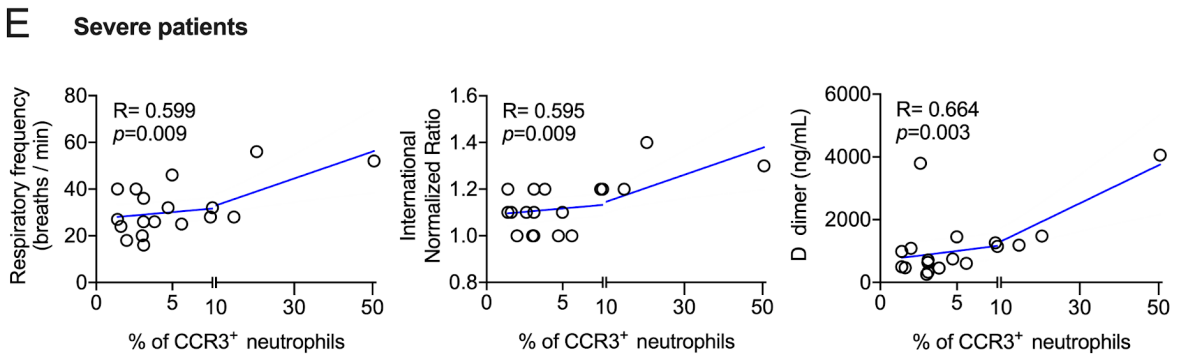

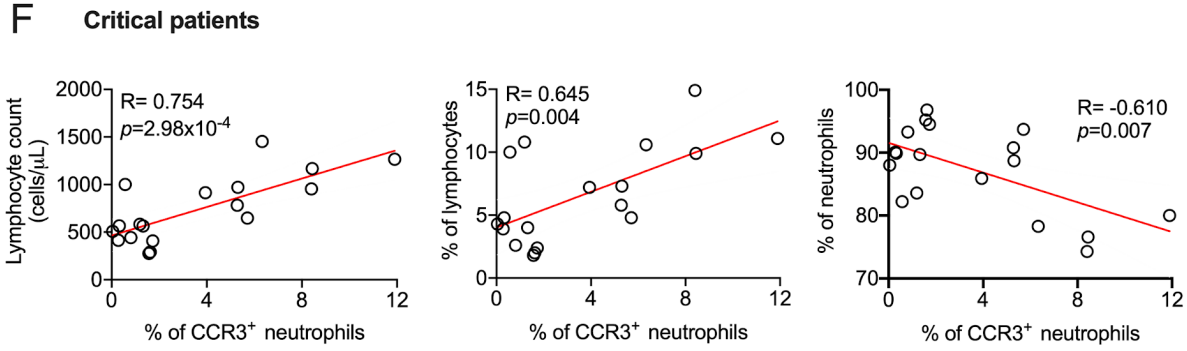

Supp. Fig. 6

Supplementary Figure 6. CCR3 and CCR10 are expressed on the surface of neutrophils isolated from COVID-19 patients, and correlate with disease severity. Blood samples were obtained from healthy donors and COVID-19 patients, then processed to analyze neutrophils by flow cytometry. (**A**) Left panel shows a representative dot-plot of neutrophils (gated on live, $CD45^+$ $CD11b^+$ $CD62L^+$ cells) isolated from the blood, and right panel shows the percentage of neutrophils in the blood of healthy donors and COVID-19 patients classified as severe or critical. (**B-D**) Left panels show representative histograms of (**B**) CD62L, (**C**) CCR3, or (**D**) CCR10 expression on the surface of blood neutrophils from healthy donors, or severe or critical COVID-19 patients. Right panels show (**B**) Median Fluorescence Intensity (MFI) of CD62L, (**C**) percentage of surface $CCR3^+$ neutrophils or (**D**) percentage of surface $CCR10^+$ neutrophils in blood from healthy donors, or severe or critical COVID-19 patients. (**A-D**) Bars represent the mean ± SE. Data was analyzed by one-way ANOVA. Significant changes are indicated by $*p \leq 0.05$, $**p \leq 0.01$, $****p \leq 0.0001$. (**E, F**) Pearson correlation between the percentage of $CCR3^+$ neutrophils and clinical parameters of patients with severe or critical COVID-19. Representative correlation plots between the percentage of $CCR3^+$ neutrophils and selected clinical parameters with statistically significant *p* values in (**E**) severe and (**F**) critical COVID-19 patients. R coefficients (95% confidence interval) and *p* values are shown.